HAL
archives-ouvertes.fr

Potential glacial-interglacial changes in stable carbon isotope ratios of methane sources and sink fractionation

Hinrich Schaefer, Michael J. Whiticar

▶ To cite this version:

Hinrich Schaefer, Michael J. Whiticar. Potential glacial-interglacial changes in stable carbon isotope ratios of methane sources and sink fractionation. Global Biogeochemical Cycles, American Geophysical Union, 2008, 22 (GB1001), 1 à 18 p. 10.1029/2006GB002889 . insu-00381062

HAL Id: insu-00381062
https://hal-insu.archives-ouvertes.fr/insu-00381062

Submitted on 11 Mar 2021

HAL is a multi-disciplinary open access archive for the deposit and dissemination of scientific research documents, whether they are published or not. The documents may come from teaching and research institutions in France or abroad, or from public or private research centers.

L'archive ouverte pluridisciplinaire **HAL**, est destinée au dépôt et à la diffusion de documents scientifiques de niveau recherche, publiés ou non, émanant des établissements d'enseignement et de recherche français ou étrangers, des laboratoires publics ou privés.

Potential glacial-interglacial changes in stable carbon isotope ratios of methane sources and sink fractionation

Hinrich Schaefer[1,2] and Michael J. Whiticar[1]

Received 9 November 2006; revised 14 June 2007; accepted 23 August 2007; published 15 January 2008.

[1] Past atmospheric methane emissions can be constrained by $\delta^{13}CH_4$ records from ice cores only if changes to source $\delta^{13}CH_4$ signatures and sink isotope effects with varying environmental and climatic conditions are accurately known. We present reconstructions of such changes based on paleodata and recent systems observations. The results are specific for budget scenarios and are reported here for two alternative types of budgets, one including aerobic methane emissions (AMP) from plants and the other type without AMP. Shifting atmospheric $\delta^{13}CO_2$ potentially led to $^{13}CH_4$ enrichment by 0.8‰ in the preindustrial Holocene (PIH) (~150–11,000 years (a) B.P.) and ~0.3–0.6‰ at the Last Glacial Maximum (LGM) (~18,000 a B.P.) relative to today. Differing distribution of C_3 and C_4 plant precursor material may account for $^{13}CH_4$ enrichment of ~0.4‰ (PIH) and ~0.6–1.1‰ (LGM). Temperature-dependent fractionation and varying methanogenic pathways in wetlands may lead to atmospheric $^{13}CH_4$ depletion by ~0.1–1.2‰. Sink fractionation today (7.4‰) is higher than during the PIH (~7.0‰) and the LGM (~5.7‰). The cumulative effect of all processes is ~0.8‰ $^{13}CH_4$ enrichment in the PIH and ~1–1.2‰ $^{13}CH_4$ depletion at the LGM. Budget reconstructions will be inaccurate if these changes are not included.

Citation: Schaefer, H., and M. J. Whiticar (2008), Potential glacial-interglacial changes in stable carbon isotope ratios of methane sources and sink fractionation, *Global Biogeochem. Cycles*, *22*, GB1001, doi:10.1029/2006GB002889.

1. Introduction

[2] The reconstruction of methane emissions in preindustrial and glacial times is critical to understand natural climate variability [*Wunsch*, 2006] and the significance of the current concentration rise of this radiatively active gas [*Prather et al.*, 2001]. Contributions from different CH_4 sources and sinks types can be constrained through isotope-based mass balances using emission rates and the $^{13}C/^{12}C$ ratio ($\delta^{13}CH_4$) of source types, as well as the fractionation caused by sinks, and comparing them to the isotope ratio of the atmosphere [*Whiticar*, 1990; *Fung et al.*, 1991; *Hein et al.*, 1997]. The first extended preindustrial $\delta^{13}CH_4$ records now become available from air occlusions of polar ice, allowing for constraints of past CH_4 budgets [*Ferretti et al.*, 2005; *Sowers et al.*, 2005; *Schaefer et al.*, 2006; *Schaefer and Whiticar*, 2007]. These studies show unexpectedly ^{13}C-rich atmospheric $\delta^{13}CH_4$ values, which were attributed to changes in emission rates of individual source types. *Schaefer et al.* [2006] and *Whiticar and Schaefer* [2007] considered the possibility that the $\delta^{13}CH_4$ of source types and sink fractionation in the past could have been different from today's values. The underlying calculations are presented in detail here. Recent advances in the field lead to slight adjustments of the values reported by *Schaefer et al.* [2006], but the main findings remain valid. The *Ferretti et al.* [2005] and *Sowers et al.* [2005] studies of the late preindustrial Holocene (PIH), assumed that there were no past changes in source $\delta^{13}CH_4$ and sink fractionation. We test this assumption by reviewing the influence of environmental parameters on each step of the CH_4 cycle (Figure 1), using knowledge of CH_4 production in modern systems in conjunction with paleorecords of climate and vegetation.

[3] The $\delta^{13}CH_4$ of methane sources is determined largely by physical and chemical parameters, e.g., reaction rates. As CH_4 production occurs in biological systems that are adapted to certain environmental conditions, it is possible that climate change rather affects geographical distribution and emission rate of a source type than its isotopic signature. For example, in a colder climate a certain wetland plant community might be reestablished further south in similar environmental conditions as before, but still produce methane with the same, or almost the same, $\delta^{13}CH_4$.

[4] In section 2 of this study, we analyze the factors that may affect the $\delta^{13}CH_4$ of natural sources under different climatic conditions. As shown in Figure 1, there are three steps in which source $\delta^{13}CH_4$ may be altered. First, we determine how changes in atmospheric $\delta^{13}C$ of CO_2, as well as vegetation patterns, influenc e the $\delta^{13}C$ of organic CH_4 precursor material. Second, we study the impact of temperature change on CH_4 production itself, specifically in wet-

[1]School of Earth and Ocean Sciences, University of Victoria, Victoria, British Columbia, Canada.

[2]Now at Laboratoire de Glaciologie et Géophysique de l'Environnement, St. Martin d'Hères, France.

Copyright 2008 by the American Geophysical Union.
0886-6236/08/2006GB002889

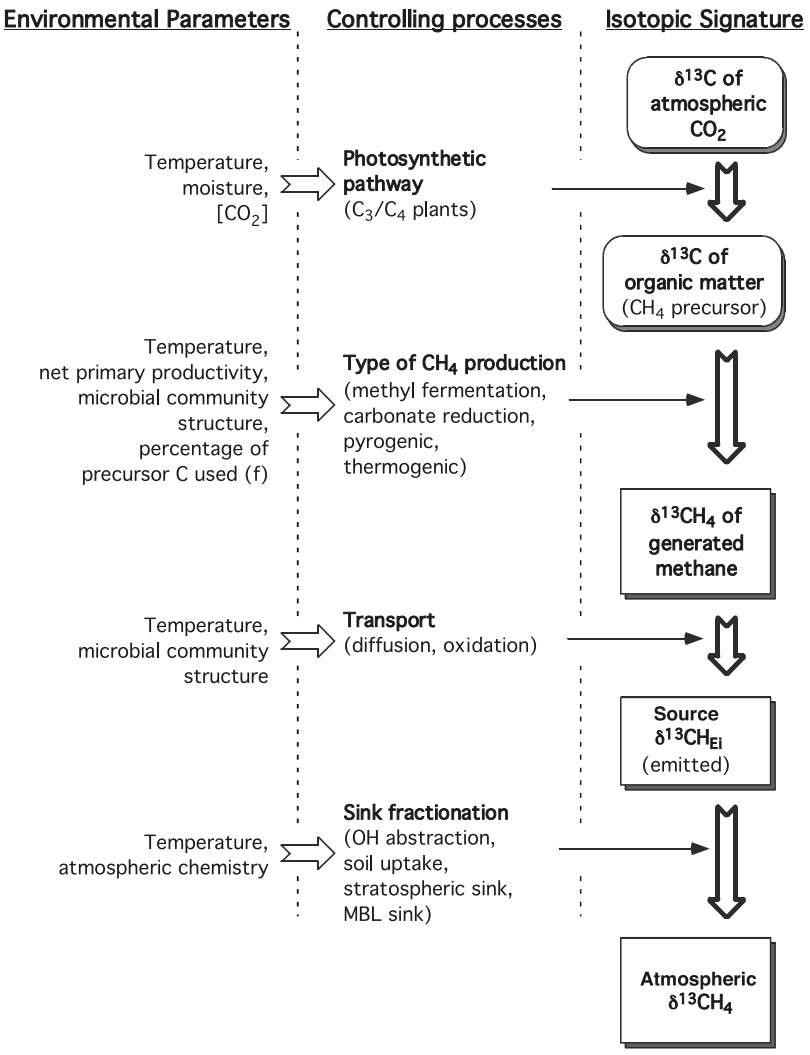

Figure 1. Methane isotope signal path. (right) Stages of the CH_4 cycle (sink processes produce CO_2 again) are shown. (center) Processes that are associated with isotopic fractionation are listed. (left) Environmental parameters influencing those processes are shown.

lands as the largest source, which is very sensitive to climate [*Kaplan*, 2002]. The main factors are the biochemical pathways of methanogenesis and their attendant isotope effects. Third, we look at partial oxidation before emission to the atmosphere. Throughout these steps, we estimate the resulting changes in atmospheric $\delta^{13}CH_4$ using isotope mass balances.

[5] In section 3, we investigate the various processes that remove CH_4 from the atmosphere, which have characteristic kinetic isotope effects (KIE). We study how the resulting fractionation varies between modern and preindustrial conditions, as well as between glacial and interglacial stages in dependence of the changing relative contributions of individual sink processes and physical changes to their fractionation coefficients.

[6] Finally in section 4, we use the above estimates to determine whether environmental influences on individual source $\delta^{13}CH_4$ and sink fractionation can indeed be neglected or if they account for the unexpected ^{13}C enrichment in the past. Any conclusions must take the large degree of uncertainty in the derived estimates into account. Uncertainty results from the multitude of factors in play, the scaling of case studies to global estimates, uncertainties in past environmental conditions and even gaps in the understanding of present-day systems. Some findings should be regarded as rather qualitative and are presented as such to stimulate further field and modeling studies.

2. The $\delta^{13}CH_4$ of Natural Methane Sources

[7] Methane is generally produced during the remineralization of organic matter under anaerobic conditions. Archaeal CH_4 production occurs in fresh water and marine sediments, soils, and in anaerobic microenvironments, e.g., animal guts. The produced $\delta^{13}CH_4$ depends mostly on the pathway of the breakdown [*Whiticar et al.*, 1986]. Other major influences are the $\delta^{13}C$ of the precursor material and the fraction of utilizable organic material consumed [*Games and Hayes*, 1976; *Whiticar*, 1996]. If the produced gas is partially oxidized during transport to the atmosphere, the

Table 1. Isotope Mass Balance for the Modern System[a]

	Total Modern		Natural Modern With AMP		Natural Modern Without AMP	
	Flux, Tg/a	$\delta^{13}C_{Ei}$,[b] ‰	Flux, Tg/a	$\delta^{13}C_{Ei}$,[b] ‰	Flux, Tg/a	$\delta^{13}C_{Ei}$,[b] ‰
Anthropogenic sources						
Rice paddies	111	−63				
Ruminants (cattle)	66	−61				
Natural gas	20	−44				
Coal	25	−37				
Biomass burning	41	−25				
Landfills	40	−55				
Natural sources						
Boreal wetlands	38	−62	38	−62	51	−62
Tropical wetlands	78	−59	78	−59	104	−55
Wild animals	15	−60	15	−60	15	−60
Termites	16	−63	16	−63	16	−63
Ocean	10	−58	10	−58	10	−58
Fresh water	4	−54	4	−54	4	−54
Gas hydrates	4	−63	4	−63	4	−63
Geologic	35	−42	35	−42	35	−42
AMP	40	−51	40	−51	-	-
Bottom-up δC_E		−54.2		−55.9		−55.7
Top-down δC_E		−54.5		−57.1		−57.1
ε_{wt}		7.4		7.4		7.4
Calculated atmospheric	545	−46.8	241	−48.5	241	−48.3
Measured atmospheric	545	−47.1[c]		−49.7[d]		−49.7[d]

[a]Source strengths from IPCC TAR, corrected to NOAA04 scale. Total modern budget is constrained by $\delta^{13}CH_4$ and deuterium/hydrogen ratios [*Whiticar and Schaefer*, 2007].
[b]From *Bréas et al.* [2001] and *Whiticar* [2000].
[c]From *Miller et al.* [2002].
[d]Calculated using ice core data from the late preindustrial Holocene [*Schaefer and Whiticar*, 2007].

residual emitted CH_4 will be more ^{13}C rich [*Whiticar and Faber*, 1986], which is here treated separately from sink processes that remove atmospheric CH_4. For any source type the above parameters will be somewhat variable, resulting in a typical $\delta^{13}CH_4$ range for this source rather than one fixed value. Nevertheless, isotope signatures can distinguish different source types [e.g., *Whiticar*, 1990].

[8] The impact of individual sources on the isotope signature of the global (or integrated) source flux ($\delta^{13}C_E$) is given by the isotope mass balance:

$$\delta^{13}C_E = \sum_1^n \left(\delta^{13}C_{Ei} \times E_i\right)/E \qquad (1)$$

where E is global emission rate in Tg/a (1 teragram = 10^{12} g); E_1 through E_n are emission rates of source types with their respective isotope values $\delta^{13}C_{Ei}$. $\delta^{13}CH_{Ei}$ values for the present are based on studies reviewed by *Bréas et al.* [2001] and given in Table 1. Modern E values are based on the IPCC TAR findings [*Prather et al.*, 2001], corrected to the NOAA04 scale [*Dlugokencky et al.*, 2005] and constrained by both $\delta^{13}CH_4$ and deuterium/hydrogen ratios [*Whiticar and Schaefer*, 2007]. The choice of emission scenario is of lesser importance for the considerations in this study. Although the source budget will influence any changes in $\delta^{13}C_E$ between different time periods, these result from a combination of changes in relative emission rates and changes in the isotopic signature of individual sources. Quantifying the latter is the purpose of this study and we use example budgets in order to delineate, and correct for, the contribution of relative emission rate changes. This will provide an estimate of the global impact of changes in $\delta^{13}C_{Ei}$ of a given source, which must be accounted for in any budget derived from paleoreconstructions. Such budget reconstructions, e.g., from ice core $\delta^{13}CH_4$ data, must therefore follow iterative steps of assigning a suitable budget scenario and correcting the associated $\delta^{13}C_E$ for $\delta^{13}CH_{Ei}$ changes until both the changes in emission rates and of $\delta^{13}C_E$ are consistent with the atmospheric $\delta^{13}CH_4$ record over a climatic transition.

[9] One budget item must be discussed in more detail, namely, aerobic methane production (AMP) in plant material, which has been reported from a laboratory study by *Keppler et al.* [2006]. Some field measurements [*Crutzen et al.*, 2006; *Sanhueza and Donoso*, 2006] and satellite data [*Bergamaschi et al.*, 2007] seem to support this process, but another laboratory study [*Dueck et al.*, 2007] failed to reproduce the results and offered an alternative explanation for the findings of *Keppler et al.* [2006]. Also, the global magnitude of AMP emissions is controversial. The original estimate by *Keppler et al.* [2006] of 150 ± 90 Tg/a, which is as high as wetland emissions (~140 Tg/a [*Kaplan*, 2002]), has been revised downward based on stable carbon isotope studies [*Ferretti et al.*, 2005] and scaling to leaf area (~53 Tg/a; ~36 Tg/a) or photosynthetic rates (~10 Tg/a) [*Parsons et al.*, 2006; *Kirschbaum et al.*, 2006], as opposed to NPP in the original work. The value we present for AMP for the modern budget in Table 1 is within the revised estimates. As the exact process that drives AMP remains poorly understood and there is a high degree of uncertainty in the global annual production rate (even whether it exists at all), we present two alternative budget scenarios for every case study throughout this paper. The first includes AMP at a rate comparable to natural wetland emissions following the reconstructions of *Houweling et al.* [2006], which must be seen as an upper estimate in light of the work by *Parsons et al.* [2006] and *Kirschbaum et al.* [2006]. In the AMP scenario, wetland emissions are reduced accordingly to keep the total source strength unchanged. The alternative scenario includes no AMP at all. Together, the alternatives provide a conservative estimate of the range in which individual source $\delta^{13}C_E$ changes can affect the total budget. One constraint on the modern budget scenarios is the necessity that the natural sources alone produce a $\delta^{13}C_E$ value that is compatible with ice core data from the period immediately preceding the industrial revolution. The modern AMP scenario gives an atmospheric $\delta^{13}CH_4$ of −48.5‰ (all $\delta^{13}CH_4$ values are reported in standard δ notation relative to VPDB standard), while the non-AMP version gives −48.3‰, if tropical wetland $\delta^{13}C_{Ei}$ is revised to −55‰ as discussed by *Schaefer et al.* [2006]. Although these values are ^{13}C depleted by ~1‰ compared to the ice data [*Ferretti et al.*, 2005; *Schaefer and Whiticar*, 2007] the agreement is reasonable given the uncertainty regarding early anthropogenic activity in the late PIH [*Ruddiman and Thomson*, 2001] and the fact that the modern natural sources are influenced by land use change.

[10] E_i values for PIH and Last Glacial Maximum (LGM) are derived from vegetation reconstructions by *Chappellaz*

et al. [1993] with two additional source types. First, ice core $\delta^{13}CH_4$ measurements from the PIH and the late glacial [*Ferretti et al.*, 2005; *Schaefer et al.*, 2006] point to a missing ^{13}C-rich source. Among several possible sources or sinks, we consider geologic, i.e., natural thermogenic emissions, a strong candidate. We chose the lower range of geologic emission estimates (35–45 Tg/a) [*Etiope and Milkov*, 2004, *Kvenvolden and Rogers*, 2005] because it is more compatible with total source strength in PIH and LGM [*Chappellaz et al.*, 1993; *Brook et al.*, 2000]. Other emissions were reduced proportionally. Second, we present scenarios including AMP as discussed above. For the PIH the assumption of equal emissions from AMP and wetlands is in agreement with the top-down calculations of *Houweling et al.* [2006] (85 Tg/a from AMP and 80 Tg/a from wetlands). However, the assumptions made here demonstrate the need for better estimates and reconstructions of emission rates. This is also seen in the fact that the combined bottom-up estimates for geologic [*Etiope and Milkov*, 2004], wetland [*Kaplan*, 2002] and AMP emissions [*Keppler et al.*, 2006] exceed total source estimates for the PIH by *Chappellaz et al.* [1993] twofold.

[11] The choice of specific, sometimes poorly constrained, emission rates will influence the reconstructed $\delta^{13}C_E$. Changes between different time periods with varying emission scenarios can therefore not be calculated directly. To isolate these effects, we quantify all potential changes in $\delta^{13}CH_4$ relative to scenarios with identical emission rates but present-day values for the tested environmental parameter.

2.1. Changes in $\delta^{13}C$ of Methane Precursor Material

[12] The $\delta^{13}C$ of organic compounds that serve as precursors in CH_4 formation influences $\delta^{13}C_{Ei}$. In turn, $\delta^{13}C$ of plant matter depends directly on the stable carbon isotope ratio of atmospheric CO_2, as well as on the photosynthetic pathway and various environmental parameters. In the following sections we estimate the impact of $\delta^{13}CO_2$ and C_3–C_4 vegetation changes on $\delta^{13}C_{Ei}$ of individual and total sources. We show that changes in $\delta^{13}CO_2$ lead to measurable ^{13}C enrichment in the past. $\delta^{13}CH_4$ changes caused by C_3–C_4 vegetation shifts are complex and seem to depend mostly on emission rates in sensitive areas. We show in the following that the estimated result is a ~0.4–0.7‰ ^{13}C depletion between glacial and interglacial conditions (in addition to further depletion caused by changes in relative emission rates).

2.1.1. Changes in Atmospheric $\delta^{13}CO_2$

[13] *Marino et al.* [1992] use plant fossils to identify a 1.1‰ ^{13}C enrichment of atmospheric $\delta^{13}CO_2$ in the PIH, and a 0.4‰ ^{13}C enrichment in glacial conditions, relative to today. The PIH result is in good agreement with $\delta^{13}CO_2$ reconstructions from ice cores [*Francey et al.*, 1999; *Smith et al.*, 1999]. However, the ice data show higher ^{13}C enrichment in the LGM (0.9‰) and a minimum (0.4‰ ^{13}C enrichment versus today) during the Younger Dryas cold period (YD) [*Smith et al.*, 1999]. It is likely that these shifts translate into changing isotopic signatures of plant material and the CH_4 derived from it. Therefore we assume that $\delta^{13}C_{Ei}$ of archaeal and pyrogenic sources change proportionately to $\delta^{13}CO_2$. The impact on atmospheric $\delta^{13}CH_4$ follows from equation (1). We calculate atmospheric ^{13}C enrichment by ~0.8‰ in the PIH and by ~0.3–0.6‰ in the LGM (for the range of reported $\delta^{13}CO_2$ changes) compared to scenarios where source $\delta^{13}C_{Ei}$ is not adjusted to past variations in $\delta^{13}CO_2$. These results are the same for scenarios with and without an AMP source.

2.1.2. Changes in C_3 and C_4 Vegetation

[14] Plants can be classified as following one of two major photosynthetic pathways, i.e., Calvin-Benson cycle (C_3) and Hatch-Slack cycle (C_4). For C_3 plants, CO_2 transport is achieved by diffusion, which causes isotopic fractionation. In contrast, C_4 plants actively transport CO_2 into the cells and consequently discriminate less against ^{13}C. Therefore C_4 plants ($\delta^{13}C$ of ~−15‰) are isotopically distinct from C_3 vegetation (~−27‰) [*Ehleringer et al.*, 1997]. The C_4 pathway is only dominant in grasslands and generally has a lower yield of carbon fixed per unit of light, but it outcompetes C_3 in warm and dry conditions, and under decreased carbon dioxide concentrations [CO_2] [*Ehleringer et al.*, 1997]. Accordingly, *Collatz et al.* [1998] model the global distribution of C_3 and C_4 plants for present, PIH and LGM. Grassland area dominated by C_4 plants increases from ~70% at the LGM to ~74% in the PIH. In modern times this proportion drops to ~57%, because of anthropogenic land conversion and rising [CO_2] [*Collatz et al.*, 1998]. One would therefore expect all sources that use C_4 material as CH_4 precursor to be more ^{13}C rich in the PIH than in the LGM than today. To determine whether this influences $\delta^{13}C_E$ one must account for the changing percentage of grasslands in global vegetation [*Prentice et al.*, 1993] and for climate-dependent CH_4 production rates in different ecosystems. The influence of C_3–C_4 vegetation change on each CH_4 source type is treated in the following sections.

2.1.2.1. Effect on Emissions From Ruminants

[15] Methane produced by ruminants is isotopically dependent on the ratio of C_3 and C_4 in their diet as shown by *Rust* [1981], *Metges et al.* [1990], *Levin et al.* [1993], *Schulze et al.* [1998] and *Bilek et al.* [2001] (Table 2). We omit data by *Metges et al.* [1990], in which $\delta^{13}CH_4$ is calculated from $\delta^{13}CO_2$, because they are inconsistent with all other data. The average value of the above studies for $\delta^{13}C_{Ei}$ from cows feeding on C_3 plants is −69‰, whereas cows eating C_4 plants produce −54‰. This 15‰ difference is almost the same as between the C_3 and C_4 feed (12‰). Significant species-dependent differences in $\delta^{13}C_{Ei}$ between cows, sheep, goats and camels [*Levin et al.*, 1993; *Schulze et al.*, 1998] are smaller than the isotopic offset between C_3 and C_4 derived CH_4 observed in all species. In addition, the difference between feed and CH_4 (~41‰) is independent of species and diet in all studies. Therefore we assume that cows are representative for all ruminants and that $\delta^{13}C_{Ei}$ produced by wild animals is directly and exclusively dependent on the C_3–C_4 proportion of their diet.

[16] Today's global average diet of domestic cattle consists of C_3 and C_4 plants at a ratio of 2.5: 1 [*Stevens and Engelkemeir*, 1988], resulting in expected ruminant $\delta^{13}C_{Ei}$ of ~−64‰. Wild animals exhibit no preference for ingesting C_3 versus C_4 plants [*Ehleringer and Monson*, 1993], so that the diet should reflect the natural abundance of the two

Table 2. The $\delta^{13}C_{Ei}$ Produced by Ruminants Depending on Diet[a]

	Source	C_4 in Diet, %	$\delta^{13}C$ Diet, ‰	$\delta^{13}C_{Ei}$, ‰	Offset Between Diet and CH_4, ‰
Cows	L	0	−27	−65.1	38.1
Cows	B	0	−28.9	−72	43.1
Cows	B	0	−28.9	−72.1	43.2
Cows	M	0	−27.1	−70.2	43.1
Cows	R	0	−27	−63.7	36.7
Cows	S	0	−27	−68.2	41.2
Cows	B	3	−27.6	−66	38.4
Cows	B	8	−25.6	−65.2	39.6
Cows	B	8	−25.6	−65.9	40.3
Cows	B	13	−23.6	−62.6	39
Cows	B	13	−23.7	−61.8	38.1
Cows	L	30	−22.8	−63.3	40.5
Cows	L	70	−17.2	−55.6	38.4
Cows	L	100	−13	−54	41
Cows	B	100	−13	−54.5	41.46
Cows	M	100	−12	−56.2	44.2
Cows	R	100	−13	−50.3	37.3
Average C_3				−68.6 ±3.5	
Average C_4				−53.7 ±2.5	
Sheep	R	0	−27.9	−68.6	40.7
Sheep	L	0	−27	−70.6	43.6
Sheep	S	0	−27	−74.4	47.4
Camels	S	0	−27	−73.5	46.5
Goats	L	0	−27	−65.2	38.2
Average					40.9 ±2.9

[a]Sources are the following: R, *Rust* [1981]; M, *Metges et al.* [1990]; L, *Levin et al.* [1993]; S, *Schulze et al.* [1998]; and B, *Bilek et al.* [2001]. Range is ± 1 standard deviation.

plant types. Using the distribution of grassland types from *Collatz et al.* [1998] and the $\delta^{13}CH_4$ reported from cows, we calculate the $\delta^{13}C_{Ei}$ emitted by wild animals as ∼−60.5‰ today, ∼−57.9‰ in the PIH and ∼−58.5‰ at the LGM (Table 3). We neglect differences between species, the effect of diet on the amount of CH_4 production [*Bilek et al.*, 2001], differing population density in various ecosystems and the low number of forest living animals (C_3 diet only). These are not expected to affect the isotopic differences between different climatic stages. There is a remarkable difference between the $\delta^{13}C_{Ei}$ of present-day wild (∼−60.5‰) and domestic animals (∼−64‰). The latter value should not be used for ruminant emissions in the past. Under unchanged climatic conditions, we estimate wild animal emissions in the PIH to be ∼2.6‰ more ^{13}C rich than today, which results from more C_4 plants at lower atmospheric [CO_2] and changes in land use. Owing to colder and drier conditions with lower [CO_2] at the LGM, we calculate animal $\delta^{13}C_{Ei}$ to be ∼0.6‰ more ^{13}C depleted than in the PIH.

2.1.2.2. Effect on Wildfire CH_4

[17] *Chanton et al.* [2000] report values between −17 and −26‰ for grass fire $\delta^{13}C_{Ei}$ (C_4) that are distinct from the range of −26 to −30‰ for forest fire $\delta^{13}C_{Ei}$ (C_3), where the respective ranges depend on combustion efficiency. Changing C_3–C_4 abundance in the past is therefore expected to influence wildfire $\delta^{13}C_{Ei}$. We calculate the percentage of C_3 and C_4 plants burned annually in wildfires in PIH and LGM using (1) paleovegetation data from *Prentice et al.* [1993], (2) natural fire frequencies for different ecosystems [*Wright and Bailey*, 1982; *DeBano et al.*, 1998], (3) CH_4 production rates in fires from *Hao and Ward* [1993], and (4) the C_3–C_4 distribution from *Collatz et al.* [1998]. The amount of wildfire CH_4 that we calculate for present day with this approach is substantially higher than estimates by *Hao and Ward* [1993], most likely due to overestimated fire frequencies. However, downscaling the results would not affect calculated $\delta^{13}CH_4$ shifts, which are the focus of this study. We present different scenarios covering the quoted ranges in fire frequency and $\delta^{13}C_{Ei}$ (Table 4). Despite these uncertainties and the resulting range of $\delta^{13}C_{Ei}$ for the PIH (∼−24.2 to −29.4‰, average −26.6‰) and LGM (∼−24.1 to −29.4‰, average −26.7‰), the calculated differences between the two time periods are< 0.3‰ for all scenarios. Using data from *Hao and Ward* [1993] today's $\delta^{13}C_{Ei}$ from biomass burning is calculated to be ∼−24.6‰, indicating a ∼2‰ ^{13}C enrichment between PIH and modern conditions.

2.1.2.3. Effect on Wetland Emissions

[18] $\delta^{13}C_{Ei}$ of wetland methane is determined by several factors, as discussed in section 2.2, but initially by the $\delta^{13}C$ of the decomposing material. Using a compilation of CH_4 emissions from different wetland types in PIH and LGM [*Chappellaz et al.*, 1993], as well as the modeled C_3–C_4 distribution in grasslands by *Collatz et al.* [1998], we estimate the $\delta^{13}C_{Ei}$ values of wetland CH_4 (Table 5). We use $\delta^{13}C_{Ei}$ = −62‰ for CH_4 derived from C_3 plants and −50‰ from C_4 plants [*Bréas et al.*, 2001]. We find that wetland CH_4 is ^{13}C-enriched by ∼2.8‰ at the LGM and by ∼0.4‰ in the PIH compared to modern values.

[19] The total contribution of C_4-derived CH_4 in the PIH is only half that in the LGM (despite higher percentage of C_4 plants in PIH grasslands), which explains the strong glacial-interglacial difference. $\delta^{13}C_{Ei}$ from C_3 dominated temperate and boreal wetlands is calculated as ∼−61.3‰ for the LGM and ∼−61.8‰ for both PIH and present (Table 5). For tropical wetlands (mixed C_3 and C_4), the estimated results are ∼−56.7‰ for the LGM, ∼−58.3‰ for PIH and ∼−59.1‰ at present.

2.1.2.4. Effect on Aerobic Methane Production

[20] The isotopic offset between AMP $\delta^{13}C_{Ei}$ in living C_3 versus C_4 plants is ∼6‰, i.e., lower than between the respective plant tissues [*Keppler et al.*, 2006]. Methane from leaf litter shows a higher offset (∼9‰), but is of minor importance for the global budget. *Keppler et al.* [2006] estimate the present-day $\delta^{13}C_{Ei}$ of total AMP as ∼−50‰ (based on emission rates in various ecosystems, which are scaled to NPP, and an assumed C_3: C_4 ratio of 60: 40). It has since been argued that AMP emissions have to be scaled to either photosynthetic rates or leaf area in order to get a realistic estimate. We therefore recalculate the present-day $\delta^{13}C_{Ei}$ of total AMP using scaling to the leaf area index (LAI) as described by *Kirschbaum et al.* [2006], as well as the ecosystem classification of *François et al.* [1998]. The revised estimate is ∼−48.9‰ (Table 6), i.e., ∼1‰ more ^{13}C rich than the number calculated after *Keppler et al.* [2006]. The conversion between slightly different ecosystem classifications in the two studies introduces very little uncertainty. For example, a recalculation of the present-day value in the classification used by *Keppler et al.* [2006] and *Kirschbaum et al.* [2006] gives $\delta^{13}C_{Ei}$ ∼−49.1‰, and is therefore indistinguishable from the value calculated with

Table 3. Influence of C_3/C_4 Vegetation on $\delta^{13}C_{Ei}$ of Natural Methane Sources[a]

	Present			PIH				LGM			
	Flux, Tg/a	C_4 Derived, %	$\delta^{13}C_{Ei}$, ‰	Flux, Tg/a	C_4 Derived, %	$\delta^{13}C_{Ei}$, ‰	$\Delta\delta$, ‰	Flux, Tg/a	C_4 Derived, %	$\delta^{13}C_{Ei}$, ‰	$\Delta\delta$, ‰
Budget Scenarios Including AMP Emissions											
AMP	42	21	−48.9	42	32	−48.5	0.4	34	30	−48.6	0.3
Tropical wetland	32	26	−59.1	44	34	−58.3	0.8	23	46	−56.7	2.4
Geologic	35		−41.8	35		−41.8	0.0	35		−41.8	0
Boreal wetland	16	4	−61.8	26	4	−61.8	0.0	2	9	−61.3	0.5
Termites	16	31	−63.0	16	20	−63.0	0.0	13	18	−63.0	0
						(−62.2)	(0.8)			(−62.7)	(0.3)
Wild animals	3	57	−60.5	12	74	−57.9	2.6	13	70	−58.5	2
Ocean	8		−58.2	8		−58.2	0.0	8		−58.2	0
Wildfire	4	48	−24.6	4	20	−26.7	−2.1	4	21	−26.6	−2
Clathrate	4		−62.5	4		−62.5	0.0	0		−62.5	0
Total	166	16	−52.5	192	22	−53.3	0.4	132	25	−50.7	0.6
Budget Scenarios Without AMP Emissions											
Tropical wetland	60	26	−59.1	71	34	−58.3	0.8	54	46	−56.7	2.4
Geologic	35		−48.8	35		−41.8	0.0	35		−41.8	0
Boreal wetland	36	4	61.8	42	4	−61.8	0.0	5	9	−61.3	0.5
Termites	16	31	−63.0	16	20	−63.0	0.0	13	18	−63.0	0
						(−62.2)	(0.8)			(−62.7)	(0.3)
Wild animals	3	57	60.5	12	74	−57.9	2.6	13	70	−58.5	2
Ocean	8		−58.2	8		−58.2	0.0	8		−58.2	0
Wildfire	4	48	−24.6	4	20	−26.7	−2.1	4	21	−26.6	−2
Clathrate	4		−62.5	4		−62.5	0.0	0		−62.5	0
Total	166	15	−55.6	192	20	−55.9	0.4	132	28	−52.9	1.1

[a]Source $\delta^{13}C_{Ei}$ adjusted for changing proportions of C_3 and C_4 precursor material [after *Collatz et al.*, 1998; *Chappellaz et al.*, 1993]. $\Delta\delta$ for individual sources is the offset between adjusted and present-day $\delta^{13}C_{Ei}$. Total $\Delta\delta$ is the offset between atmospheric $\delta^{13}CH_4$ values in the adjusted mass balance and one using present-day source $\delta^{13}C_{Ei}$.

Table 4. Methane Emissions From Wildfires and Its $\delta^{13}C_{Ei}$ During LGM and PIH Emission Rates for Each Ecosystem Calculated From Literature Estimates[a]

	Biomass					CH_4 Emissions			
	LGM, Pg C	PIH, Pg C	1/Fire Frequency	Fraction Burned	CH_4/Biomass, g/kg	LGM, Tg/a	LGM Average, Tg/a	PIH, Tg/a	PIH Average, Tg/a
Grassland									
Warm grass and shrubland	10.3	13	0.1–0.5	0.81	1.5	1.2–6.2	2.1	1.6–7.9	2.6
Cool grass and shrubland	7.2	5.7	0–0.1	0.81	1.5	0.3–4.4	0.6	0.3–3.5	0.5
Wooded tundra	4.2	5.2	0	0.81	1.5	0	0	0	0
Tundra	6.48	5.7	0	0.81	1.5	0	0	0	0
Tropical dry forest and savanna	84.6	79.1	0.1–0.3	0.81	1.5	10.3–33.9	17.1	9.6–31.7	16.0
Tropical forest									
Tropical rain forest	176	164	0	0.45	9.3	0	0	0	0
Tropical seasonal forest	105	102.2	0	0.45	9.3	0	0	0	0
Warm mixed forest	87	62	0–0.3	0.45	9.3	14.6–121.4	26.0	10.4–86.5	18.5
Temperate and boreal forest									
Temperate deciduous forest	35	58	0.1	0.45	6.1	9.6–13.7	11.3	15.9–22.7	18.7
Cool mixed forest	19	49	0–0.2	0.45	6.1	0.1–8.7	0.3	0.4–22.4	0.7
Cool conifer forest	10.1	50.4	0.0–0.3	0.45	6.1	0.9–9.2	1.6	4.3–46.1	7.9
Taiga	22.6	88.7	0	0.45	6.1	0	0	0	0
Northern taiga	6.5	11.5	0	0.45	6.1	0	0	0	0
Cold mixed forest	5	7	0	0.45	6.1	0	0	0	0
Cold deciduous forest	8.7	22.6	0.01	0.45	6.1	0.2	0.2	0.6	0.6
Northern cold deciduous forest	2.6	10.4	0–0.1	0.45	6.1	0–0.4	0.0	0.1–1.7	0.1
Xerophytic wood, shrublands	55.4	46.3	0–0.1	0.65	6.1	5.0–11.0	6.9	4.2–9.2	5.8
Global C_4						8–31	14	9–32	14
Global C_3						34–178	52	39–201	57
$\delta^{13}C_{Ei}$, ‰						−24.1 to −29.4	−26.6	−24.2 to −29.4	−26.7

[a]The $\delta^{13}C_{Ei}$ for pure C_3 and C_4 vegetation is from *Chanton et al.* [2000]. Biomass estimates are from *Prentice et al.* [1993]; annual fire frequencies are after *Wright and Bailey* [1982] and *DeBano et al.* [1998]; fraction burned and CH_4 produced per burned biomass is from *Hao and Ward* [1993].

Table 5. Methane Emissions From Different Wetlands and Their $\delta^{13}C_{Ei}$ in Dependence of C_3 and C_4 Vegetation[a]

	Emissions								
	LGM, Tg/a			PIH, Tg/a			Present, Tg/a		
	Total	C_3	C_4	Total	C_3	C_4	Total	C_3	C_4
Temperate and boreal									
Boreal/conifer forest	1	1		17	17		15	15	
Tundra	0	0		8	8		8	8	
Temperate broad-leaved forest	5	5		20	20		9	9	
Open conifer woodlands	2	1.3	0.7	6	3.78	2.22	6	4.38	1.62
Total	8	7	1	51	49	2	38	36	2
$\delta^{13}C_{Ei}$	−61.3‰			−61.8‰			−61.8‰		
Tropical									
Tropical moist forest	16	16		33	33		27	27	
Tropical scrub/woodlands	14	9.1	4.9	27	17.01	9.99	25	18.25	6.75
Grassland	33	9.9	23.1	21	5.46	15.54	21	9.66	11.34
Semidesert/steppe	2	0.6	1.4	2	0.52	1.48	2	0.92	1.08
Desert	3	0.9	2.1	2	0.52	1.48	2	0.92	1.08
Total	68	37	32	85	57	28	77	57	20
$\delta^{13}C_{Ei}$	−56.7‰			−58.3‰			−59.1‰		
Total	76	44	32	136	105	31	115	93	22
Percentage		58%	42%		77%	23%		81%	19%
$\delta^{13}C_{Ei}$	−57.2‰			−59.6‰			−60.0‰		

[a]Emission estimates from *Chappellaz et al.* [1993]. The $\delta^{13}C_{Ei}$ for C_3 wetlands is taken as −62‰; for C_4 wetlands it is taken as −50‰ [*Bréas et al.*, 2001].

the *François et al.* [1998] classification. Estimates for the PIH and LGM are subject to more uncertainty because LAI for tropical forests [*Harrison and Prentice*, 2003] as well as season length and hours of sunshine, which control emission rates [*Keppler et al.*, 2006; *Kirschbaum et al.*, 2006], may have been different because of changes in cloud cover and latitudinal shifts of sources. For simplicity, we use the modern values throughout. We calculate a $\delta^{13}C_{Ei}$ of ∼−48.5‰ for the PIH and ∼−48.6‰ for the LGM. These results suggest that a higher proportion of C_4 precursor material enriches AMP in ^{13}C by ∼0.4‰ in the PIH and by ∼0.3‰ at the LGM, compared to today.

2.1.2.5. Effect on Termite Emissions

[21] *Tyler et al.* [1988] compare the $\delta^{13}C_{Ei}$ produced by termites in various habitats. They find no correlation between diet, specifically C_3 and C_4 plants, and produced $\delta^{13}C_{Ei}$, not even within a single species. This surprising result suggests that past C_3–C_4 changes do not influence $\delta^{13}C_{Ei}$ of termite emissions. Considering that all other CH_4 sources display such a dependence on plant species, we explore the potential variation in termite $\delta^{13}C_{Ei}$ if there were a direct correlation to the precursor material. We use paleovegetation data from *Prentice et al.* [1993] and ecosystem-specific CH_4 production rates from *Zimmerman et al.* [1982]. We calculate ∼−62.2‰ for the PIH and ∼−62.7‰ for the LGM, compared to the measured modern value of −63.0‰ (Table 3). We show below that such postulated changes have insignificant impact on $\delta^{13}C_E$.

2.1.2.6. Effect on $\delta^{13}C_E$

[22] The $\delta^{13}C_{Ei}$ of marine and thermogenic sources is not affected by vegetation change at all, because they do not utilize terrestrial plant material as a precursor. Also, termite

Table 6. The $\delta^{13}C_{Ei}$ of AMP in LGM, PIH, and Present in Dependence of C_3 and C_4 Vegetation[a]

	Present				PIH				LGM			
	Area, 10^9 ha	Emission, Tg/a	C_3 Derived, Tg/a	C_4 Derived, Tg/a	Area, 10^9 ha	Emission, Tg/a	C_3 Derived, Tg/a	C_4 Derived, Tg/a	Area, 10^9 ha	Emission, Tg/a	C_3 Derived, Tg/a	C_4 Derived, Tg/a
Semidesert	4.8	4.2	3.0	1.1	1.72	1.5	0.9	0.6	3.08	2.7	1.7	0.9
Grassland	3.25	7.9	3.6	4.3	5.66	13.8	3.6	10.2	4.47	10.9	3.3	7.6
Needleleaf forest	1.37	2.9	2.9		1.91	4.0	4.0		1.13	2.4	2.4	
Broadleaf evergreen forest	1.75	18.8	16.2	2.5	1.47	15.8	12.8	2.9	0.95	10.2	8.4	1.8
Broadleaf deciduous forest	1.04	3.4	3.4		2.18	7.2	7.2		2.39	7.9	7.9	
Crops	1.41	4.6	3.9	0.8								
Total	13.6	41.7	33.1	8.7	12.94	42.2	28.5	13.7	12.02	34.0	23.6	10.3
Percentage			79.2%	20.8%			67.6%	32.4%			69.6%	30.4%
$\delta^{13}C_{Ei}$		−48.9				−48.5				−48.6		

[a]Estimates of biome areas from *Francois et al.* [1998], emission rates scaled to leaf area index after *Kirschbaum et al.* [2006]. C_3–C_4 distribution follows *Collatz et al.* [1998]. The $\delta^{13}C_{Ei}$ for pure C_3 and C_4 derived methane from *Keppler et al.* [2006].

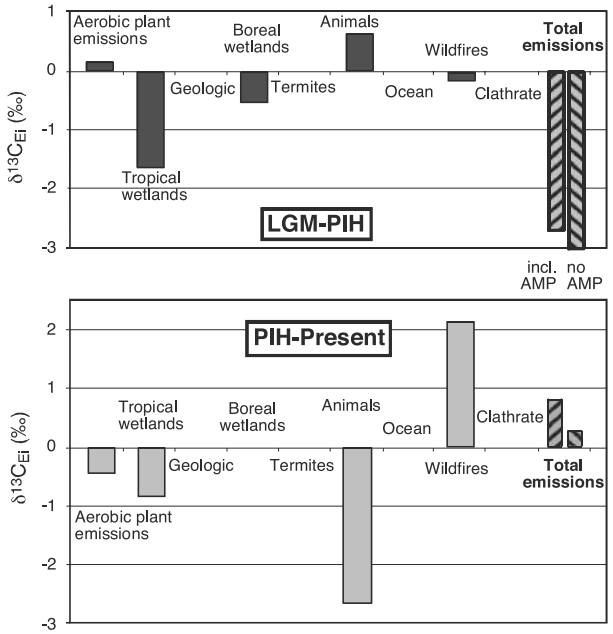

Figure 2. Changes in $\delta^{13}C_{Ei}$ of methane sources between LGM, PIH, and today. Estimates are derived from published emission rates (Table 3) and paleodata for individual sources. Negative values denote ^{13}C depletion (top) in PIH relative to LGM and (bottom) for the present relative to PIH. Estimates for total emission changes ($\delta^{13}C_E$) are given for scenarios with, and without, AMP emissions. See text for discussion of uncertainties.

emissions have been shown not to reflect the isotopic signature of their precursor material [*Tyler et al.*, 1988]. In contrast, we have demonstrated that the other terrestrial archaeal sources and biomass burning experience significant $\delta^{13}C_{Ei}$ changes between LGM, PIH and present, because of C_3-C_4 shifts (Figure 2 and Tables 3 and 7). The largest estimated changes for individual source types occur from PIH to present in animal (~2.6‰ ^{13}C depletion) and wildfire emissions (~2.1‰ ^{13}C enrichment), while tropical wetlands and AMP become more ^{13}C depleted by ~0.8‰ and ~0.4‰, respectively. From LGM to PIH boreal wetlands become moderately ^{13}C depleted (~0.5–0.6‰) and animal emissions become more ^{13}C rich by a similar amount. Tropical wetlands become ^{13}C depleted by ~1.6‰. AMP becomes enriched by ~0.1‰ and wildfires depleted by the same amount. These calculated results show that the $\delta^{13}C_{Ei}$ of source types cannot be assumed to be constant over climatic transitions and that the same environmental changes cause ^{13}C enrichment in some source types but depletion in others.

[23] We calculate the total effect of C_3-C_4–dependent changes according to equation (1), relative to scenarios with the same flux rates but unchanged, present-day $\delta^{13}C_{Ei}$ values. We quote all estimates for a budget that includes AMP emissions, followed by the equivalent estimate in a non-AMP scenario in parentheses. We estimate that in the PIH changes in C_3-C_4 vegetation lead to moderate ~0.4‰ (~0.4‰) ^{13}C enrichment of atmospheric $\delta^{13}CH_4$. In the LGM, the enrichment is stronger at ~0.6‰ (~1.1‰).

[24] The reconstructed atmospheric $\delta^{13}CH_4$ values depend on the emission scenarios (Figure 3). In addition, the calculated values carry a large degree of uncertainty because of poorly constrained data and assumptions. However, our main interest is to quantify the relative changes in $\delta^{13}C_E$ between LGM, PIH, and present. These are better constrained than the absolute values because errors resulting from various assumptions probably are consistent for all periods.

[25] The most interesting finding is a lack of correlation between global abundance of C_3 versus C_4 vegetation and $\delta^{13}C_E$. Between PIH and present, when C_4 plants decrease drastically relative to C_3 vegetation (−17%), our study predicts a fairly small impact on $\delta^{13}C_E$, i.e., ~−53.3‰ in the PIH versus ~−52.5‰ at present (~−55.9‰ versus ~−55.6‰; here and in the following values in parentheses are for non-AMP scenarios) (Table 3 and Figure 2). In contrast, between LGM with $\delta^{13}C_E$ ~−50.7‰ (~−52.9‰) and PIH, when the C_3-C_4 distribution changes by only 4%, we calculate ^{13}C depletion of ~2.6‰, (~3.0‰), which would strongly affect ice core $\delta^{13}CH_4$ records. The depletion is unexpected, because the PIH environment hosts more ^{13}C-rich C_4 plants [*Collatz et al.*, 1998]. However, the contribution of C_4-derived CH_4 to the total source in the PIH is only ~22% (~20%), i.e., lower than during the LGM with 25% (28%) (Table 3). Therefore $\delta^{13}C_E$ does not merely

Table 7. Influence of Individual Sources on the Isotopic Offset Between LGM and PIH[a]

	Change $\delta^{13}C_{Ei}$ to LGM Values		Change Source Contributions to LGM Values	
	$\delta^{13}C_{Ei}$ Offset (LGM-PIH), ‰	$\Delta\delta^{13}C_E$, ‰	Change in Relative Emission Rate, %	$\Delta\delta^{13}C_E$, ‰
Budget Scenarios Including AMP Emissions				
AMP	−0.1	0.0	−4	0.2
Tropical wetland	1.6	0.4	6	0.3
Geologic	0	0	−8	0.9
Boreal wetland	0.5	0.1	+12	1.2
Termites	0	0	−1	−0.1
Wild animals	−0.6	0	−4	−0.2
Ocean	0	0	−2	−0.1
Wildfires	0.1	0	−1	0.2
Clathrates	0	0	+2	0.2
All sources		0.4		2.5
Basic LGM scenario		2.6		2.6
Budget Scenarios Without AMP Emissions				
Tropical wetland	1.6	0.6	−4	−0.1
Geologic	0	0	−8	1.1
Boreal wetland	0.5	0.1	+18	1.3
Termites	0	0	−2	−0.1
Wild animals	−0.6	0	−4	−0.1
Ocean	0	0	−2	0
Wildfires	0.1	0	−1	0.3
Clathrates	0	0	+2	0.1
All sources		0.7		2.3
Basic LGM scenario		3.0		3.0

[a]PIH isotope mass balance recalculated using LGM values for individual sources in order to evaluate the impact of reconstructed changes in source $\delta^{13}C_{Ei}$ and relative emission rates on $\delta^{13}C_E$, compared to the unaltered reconstructed PIH balance ($\Delta\delta^{13}C_E$).

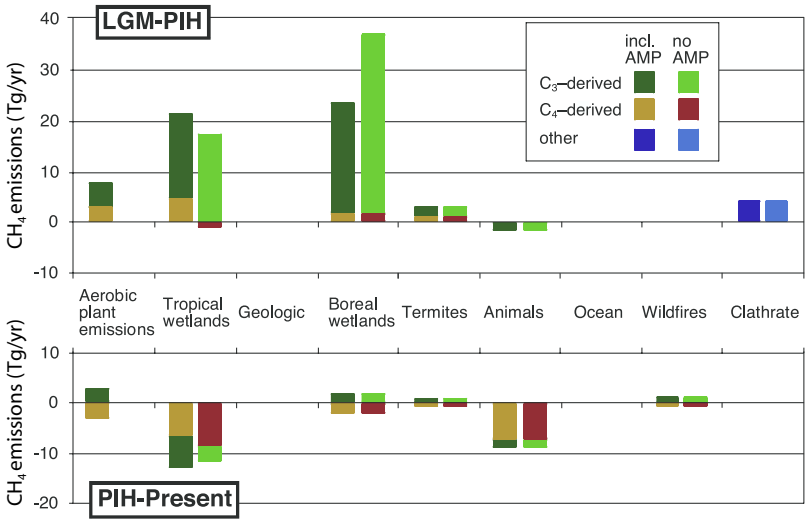

Figure 3. Changes in emission rates of CH_4 sources between LGM, PIH, and today. Emission rates are calculated after *Chappellaz et al.* [1993] (no uncertainty range reported) and other literature data (see text). Sources are listed according to total emission strength. Estimates are given for budgets with, and without, AMP emissions. (top) Between LGM and PIH, C_3-derived sources increased strongly because of higher NPP especially in high latitudes. (bottom) Between PIH and modern conditions most terrestrial natural methane sources decrease because of land conversion.

reflect the global abundance of C_3 and C_4 plants, but is controlled by their distribution in specific, climate sensitive ecosystems with high methane emission rates.

[26] To identify the sources that cause the remarkable LGM-PIH difference, we recalculate the PIH mass balance using LGM values of $\delta^{13}C_{Ei}$ for individual source types (Table 7). The results show that the change in $\delta^{13}C_{Ei}$ of tropical wetlands accounts for ~0.4‰ (~0.6‰) of the total ~2.6‰ (~3.0‰) depletion, and boreal wetlands for ~0.1‰ (~0.1‰). The effects of all other sources (including postulated changes to termite $\delta^{13}C_{Ei}$) are negligible. In total, the glacial-interglacial changes in $\delta^{13}C_{Ei}$ of source types due to C_3–C_4 shifts cause ^{13}C depletion of $\delta^{13}C_E$ of only ~0.4‰ (~0.7‰) (Table 7).

[27] To explain the remainder of the LGM-PIH $\delta^{13}C_E$ offset that cannot be attributed to changes in $\delta^{13}C_{Ei}$ of individual sources, we also recalculate the PIH mass balance with LGM emission rates (as percent of total emissions) for each source type (Table 7). Two sources have a strong impact, namely, the ~8% (~8%) relative decrease of geologic emissions that causes ~0.9‰ (~1.1‰) ^{13}C depletion, compared to the total of ~2.6‰ (~3.0‰), as well as the ~12% (~18%) increase of boreal wetlands (including temperate regions) that causes ~1.2‰ (~1.3‰) ^{13}C depletion. It is notable that a change of only 1% in relative wildfire emission rates causes ~0.2‰ (~0.3‰) depletion, underlining the strong impact this source with its extreme $\delta^{13}C_{Ei}$ has on the isotope budget. Changing all source percentages accounts for ~2.5‰ (~2.3‰) of the total offset (Table 7). On one hand, these findings fit the conventional interpretation that changing emission rates determine atmospheric $\delta^{13}CH_4$ (Figure 3). On the other hand, the impact of boreal wetland CH_4, which is just one of several microbial sources, is larger than might be expected, because of the glacial shutdown of C_3-derived CH_4 from boreal wetlands. The subsequent strong increase of this source causes the percentage of C_4-derived CH_4 to drop in the PIH (Tables 3 and 5). Therefore the total contribution of C_3 and C_4 derived CH_4 does play a significant role, but it is driven by changes in emission rates of specific sources (Figure 3). These findings suggest that wetlands with different vegetation types and in different latitudinal belts must be considered separately in isotope budgets in order to avoid significant errors.

[28] The uncertainty of the estimates given above is difficult to quantify. A major factor that affects the results is the choice of source budget. We have presented alternative estimates for budgets with and without an AMP source and see that the two differ substantially in the reconstructed changes of $\delta^{13}C_E$ between climatic changes. For example, the AMP budget results in a $\delta^{13}C_E$ difference between LGM and PIH of ~2.6‰, i.e., 0.4‰ smaller than for the non-AMP budget (~3.0‰). In a source scenario with AMP scaled to NPP instead of LAI, the LGM-PIH difference due to C_3–C_4 changes is only ~1.7‰ (calculation not shown). In a source scenario that includes neither AMP nor geologic emissions the LGM-PIH difference is ~1.9‰ [*Schaefer*, 2005]. In the latter case, it is noteworthy that the vegetation model of *Kaplan et al.* [2004] predicts a similar isotope offset between LGM and PIH for a comparable source budget. Despite the discrepancies, it should be noted that all four of these case studies predict ^{13}C depletion between LGM and PIH as the result of C_3–C_4 changes at a magnitude that is measurable in ice cores.

[29] A second and more serious source for errors in reconstructed $\delta^{13}C_E$ is uncertainties in the calculated changes of $\delta^{13}C_{Ei}$ for individual sources (Table 3). The calculations are based on the vegetation reconstructions by *Chappellaz et al.* [1993] and the modeled C_3–C_4 changes of *Collatz et al.* [1998]. Neither of these studies quantifies the

associated errors. Consequently, we cannot present a formal error analysis for our derived values. Instead, we investigate the general uncertainty associated with vegetation models. Then we conduct a sensitivity study based on the findings.

[30] *Collatz et al.* [1998] use a very simple model to determine the predominance of C_3 or C_4 vegetation, which is purely based on the specific crossover temperature at which one of the pathways starts to outcompete the other. The area of C_4 vegetation is either reported as global potential, i.e., all C_4 favorable regions including those covered by woody vegetation, or as percentage of grasslands, which are assumed to cover 25% of global land area. A later study by the same group [*Still et al.*, 2003] used a more sophisticated approach that accounts for croplands and multistoried vegetation. They arrive at a higher global surface area covered by C_4 plants that would, applying the *Collatz et al.* [1998] calculation for C_4 grassland area, result in a 24% increase of modern C_4 grassland area compared to the original study. This would suggest a larger role of C_4 vegetation in the global methane cycle and therefore a higher impact of vegetation changes between climatic stages. However, the increase is mostly due to improved C_4 quantification in wooded areas, where the *Still et al.* [2003] model allows for mixed C_3 and C_4 vegetation. The two studies may in fact be quite comparable in predicted C_4 grassland area, which are the basis for estimates presented here. In addition, the relative changes between climatic stages can be expected to be insensitive to the absolute values.

[31] *Heimann et al.* [1998] and *Cramer et al.* [1999] investigated the general range of uncertainty between different vegetation models. For the same input they found that modeled NPP deviated by ±11% (1 SD, six models) and ±19% (sixteen models), respectively. Furthermore, *Hallgren and Pitman* [2000] studied the sensitivity of a single vegetation model (BIOME 3) to the range of reported values for input parameters. They found that the photosynthesis parameterization, which is essential for determining C_3 or C_4 predominance, is particularly sensitive when the extremes of reported literature values were used instead of an initially adopted intermediate value. The difference between the generated vegetation maps is quantified by the global κ statistic, where 1 means perfect agreement and 0 that agreement is no better than random. For single parameters κ values reach up to 0.42. The average change in κ for 12 parameters is 0.85 and 0.89 for minimum and maximum literature values.

[32] Finally, the climatic boundary conditions influence the magnitude of the modeled vegetation change. *Harrison and Prentice* [2003] quantified the differences in model output of the BIOME 4 vegetation model for 17 climate model reconstructions of the LGM. They found that total grassland area in the Northern hemisphere and intertropics varied by ±10% (1 SD) (±15% for LGM climate simulations with modern CO_2 levels). Modeled NPP in global forested areas varied only by ±2%. Comparisons of the vegetation maps derived from the model runs with paleovegetation proxies indicate that in general the models underestimate the importance of climate change [*Harrison and Prentice*, 2003].

[33] The uncertainty associated with modeled paleovegetation changes is on the order of ±10–20% for each of (1) vegetation algorithms, (2) knowledge of physiological parameters and (3) climatic forcing. Consequently, it is necessary to test the sensitivity of our reconstructions to large errors in atmospheric $\delta^{13}CH_4$ introduced by the vegetation models. We have already presented calculations of $\delta^{13}C_E$ for our LGM and PIH scenarios with modern source $\delta^{13}C_{Ei}$ values (Table 3). These constitute a sensitivity test for the C_3–C_4 reconstructions at an error margin of minus 100%, i.e., assuming that the reconstructed changes in $\delta^{13}C_{Ei}$ are 100% too high and correcting for the whole difference to the original (modern) value. The effect on the calculated $\delta^{13}C_E$ value ranges from 0.4‰ in the PIH up to 1.1‰ at the LGM (without AMP emissions). Similarly, we have presented a minus 100% error estimate for the glacial-interglacial difference by recalculating the PIH budget with glacial $\delta^{13}C_{Ei}$ values (Table 7) and found that the impact on $\delta^{13}C_E$ is 0.4‰ in an AMP scenario and 0.7‰ without AMP. Furthermore, to test the model sensitivity, we calculate the difference in $\delta^{13}C_E$ of the LGM assuming the glacial-interglacial $\delta^{13}C_{Ei}$ difference of C_3–C_4–dependent sources varied by (1) ±25%, (2) ±50% and (3) ±100%. In the budget scenario including AMP the resulting changes in $\delta^{13}C_E$ are (1) ±0.05‰, (2) ±0.1‰, and (3) ±0.2‰, respectively. While such error margins for $\delta^{13}C_E$ may be negligible given the precision of ice core analyses, the errors in a non-AMP budget scenario are larger and amount to (1) ±0.15‰, (2) ±0.3‰ and (3) ±0.6‰, respectively.

2.2. Isotopic Fractionation During CH_4 Production

[34] In contrast to wetland emissions, whose $\delta^{13}C_{Ei}$ is subject to a complex variety of environmental influences, emissions from sources such as wildfires or intestinal tracts of ruminants come from special microenvironments, where atmospheric conditions do not influence their emitted $\delta^{13}C_{Ei}$. Other sources such as AMP are not associated with isotope effects [*Keppler et al.*, 2006]. Wetlands are the largest natural CH_4 source and are strongly climate-dependent [*Kaplan*, 2002; *van Huissteden*, 2004]. We therefore focus our study of changing isotopic fractionation under different climatic conditions on wetlands. In the following, we investigate the influence of temperature changes on fractionation coefficients, the dominance of methanogenic pathways, and the fraction of precursor material utilized. Although quantitatively many of these effects are poorly known, we show that the glacial wetland source is expected to be more ^{13}C depleted with potentially measurable impact on atmospheric $\delta^{13}CH_4$.

[35] In wetlands, CH_4 is produced either by methyl fermentation (MF) or carbonate reduction (CR) [*Whiticar et al.*, 1986]. Both are associated with KIE, which leads to ^{13}C depletion of the produced CH_4 relative to the precursor plant material. According to *Blair et al.* [1993], for the narrow range defined by glacial-interglacial changes, the temperature dependence of the fractionation coefficient α_{CR} (defined as the ratio of the reaction rates for $^{12}CH_4$ and $^{13}CH_4$) associated with CR is

$$\ln \alpha_{CR} = (23/T) - 0.022 \quad (2)$$

where T is absolute temperature. For the current global mean temperature of ~15°C, equation (2) gives α_{CR} = 1.060. In comparison, the LGM value is 1.062; assuming that mean terrestrial temperature is 7°C lower [*Collatz et al.*, 1998]. Accordingly, CR derived CH_4 would be ^{13}C depleted by ~1.8‰ at the LGM (assuming otherwise identical conditions). This is in general agreement with the findings of *Whiticar* [1996, 1999] and the CR temperature sensitivity reported by *Botz et al.* [1996], which results in slightly lower depletion of ~1.5‰. The equilibrium curve for the offset between CO_2 and CH_4 predicts a larger depletion (~2.6‰), as do empirical data from marine and freshwater sediments (~2.8‰ and ~6‰, respectively [*Whiticar et al.*, 1986; *Whiticar*, 1999]). This may indicate that these empirical relationships between T and $\delta^{13}C_{Ei}$ include not only the enzymatic temperature sensitivity but also factors like substrate availability or microbial community structure. This would make them a better analogy for the LGM scenario than the theoretical $T - \alpha$ correlation [*Blair et al.*, 1993; *Botz et al.*, 1996].

[36] We are not aware of studies that derive a temperature relationship for α_{MF}, but *Fey et al.* [2004] observe strong ^{13}C depletion in MF-derived CH_4 at 10°C (−28‰) compared to 37°C (−21‰) in rice paddy soils. The authors attribute this to an increase in α_{MF} and higher acetate availability (a major CH_4 precursor in MF) in colder conditions. It is speculative to use these findings as indicative for (1) natural wetlands and (2) glacial-interglacial climate change, but taken at face value ~2.9‰ ^{13}C depletion at the LGM would be expected by analogy. Several additional influences must be taken into account. First, *Fey et al.* [2004] find that the ratio of CH_4 produced by CR versus MF increases at lower temperatures. The higher fractionation during CR would lead to additional ^{13}C depletion of wetland CH_4 at the LGM. Second, the temperature sensitive KIE of microbial CH_4 oxidation [*Tyler et al.*, 1994] could lead to ^{13}C enrichment of emitted wetland CH_4 under LGM conditions. Third, substrate availability, the fraction of precursor material consumed and the structure of microbial communities also influence $\delta^{13}C_{Ei}$. The impact of the latter three factors on the produced $\delta^{13}C_{Ei}$ may be captured by present-day field studies on temperature effects. However, a different correlation to temperature for past conditions cannot be ruled out.

[37] *Bellisario et al.* [1999] observe correlation between ^{13}C enrichment and flux rates from wetlands in Manitoba and conclude that a higher proportion of MF at high-nutrient sites increases CH_4 production. It has since been suggested [*MacDonald et al.*, 2006] that boreal peatlands that developed since the LGM started as minerotrophic systems that emit ^{13}C-rich CH_4, thus contributing to the ^{13}C enrichment observed in ice samples from the late glacial period [*Schaefer et al.*, 2006]. The following evolution of the peatlands to ombrotrophic systems would have been associated with gradual ^{13}C depletion of this source to modern values. The hypothesis remains speculative but highlights the problem that during periods of climate and vegetation change processes may occur that are not captured by field and modeling studies of the modern system.

[38] With current knowledge, CH_4 production in wetlands is too complex to permit a robust estimate of past $\delta^{13}C_{Ei}$ variability. Nevertheless, the evidence discussed above suggests a significant difference between glacial and interglacial wetland $\delta^{13}C_{Ei}$. For further quantification, we note that wetland production in the LGM occurs to ~70% in the tropics and ~30% in temperate zones [*Chappellaz et al.*, 1993]. We assume temperature differences between LGM and today of 4°C in the tropics, 7°C in midlatitudes and 10°C in northern latitudes. Using the associated changes in α values for methanogenesis and oxidation, we estimate that LGM wetland $\delta^{13}C_{Ei}$ is more ^{13}C depleted than in the PIH by ~0.3–1.1‰, depending on the MF derived fraction (f_{MF}) relative to CR production. A good estimate may be ~0.9‰ for f_{MF} = 0.7. If f_{MF} was lower, as suggested by findings of *Fey et al.* [2004], then wetland $\delta^{13}CH_4$ depletion would be significantly higher, e.g., an additional ~1.5‰ at f_{MF} = 0.65.

[39] The effect of changing wetland $\delta^{13}C_{Ei}$ on the methane budget can be calculated according to equation (1). Again, we are considering two global budget scenarios with and without AMP and compare these to the same emission budgets with unchanged wetland $\delta^{13}C_{Ei}$ values. We find that temperature-dependent fractionation leads to very minor ^{13}C depletion of $\delta^{13}C_E$ in the LGM of ~0.1–0.2‰ for the AMP scenario and somewhat higher depletion (~0.1–0.5‰) in the non-AMP scenario. With the additional contribution from CR the change would be ~0.3–0.5‰ with AMP and ~0.8–1.2‰ without AMP. This result suggests that glacial-interglacial temperature changes have an impact on the CH_4 isotope mass balance that is detectable in ice core measurements.

2.3. Net to Gross CH_4 Production Ratio

[40] In modern wetlands the net to gross (N/G) production ratio is ~0.6, i.e., ~40% of the generated CH_4 is oxidized during transport [*Walter and Heimann*, 2000] while the remaining portion, which is emitted to the atmosphere, becomes enriched in ^{13}C. However, oxidation rates (Q_{10} values) are about half as sensitive to temperature change as rates of methanogenesis [*Segers*, 1998]. Accordingly, we calculate that the N/G ratio in the LGM could have been ~0.53. The Rayleigh equation then predicts ~7‰ ^{13}C enrichment of wetland CH_4 compared to today. However, this was likely not the case because CH_4 oxidation is much more strongly controlled by transport mechanism [*Chanton*, 2005], microbial community structure, previous CH_4 exposure of soil layers and actual CH_4 levels than it is by temperature [*Segers*, 1998]. Most importantly, no relative change of oxidation versus production was observed in a field experiment with warming plots [*Moosavi and Crill*, 1998]. This is consistent with the finding that CH_4 production and consumption potentials do not control ecosystem CH_4 flux [*Bellisario et al.*, 1999]. We therefore do not consider an effect of changing N/G ratios on wetland $\delta^{13}C_{Ei}$. In contrast, temperature-dependent changes in α_{ox} partly counter those of CH_4 formation (see above).

3. Sink Fractionation

[41] Methane removal from the atmosphere is commonly grouped in three sinks: abstraction with hydroxyl radicals (OH·) in the troposphere [e.g., *Saueressig et al.*, 2001], soil

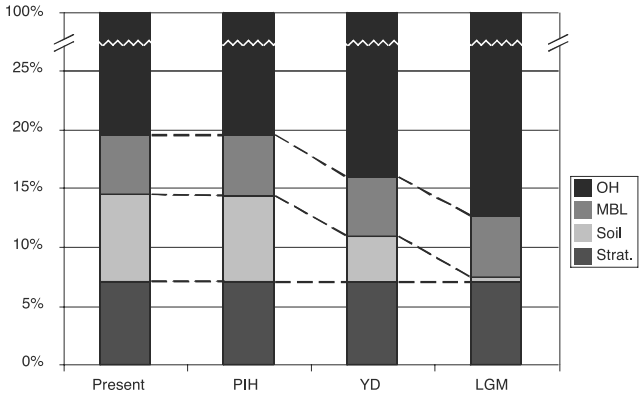

Figure 4. Relative contribution of sink processes from LGM to present. For scenarios without MBL sink, F_{soil} and F_{strat} remain as shown (i.e., the difference is negligible), while an increase in F_{OH} compensates for the missing sink (note scale break).

uptake [e.g., *Ridgwell et al.*, 1999], and stratospheric removal [e.g., *Rice et al.*, 2003]. Recently, a fourth sink has been inferred from time series of atmospheric isotope measurements and attributed to removal of CH_4 in the marine boundary layer (MBL) through reaction with chlorine [*Allan et al.*, 2005]. Each sink removes $^{12}CH_4$ preferentially and enriches the atmosphere in $^{13}CH_4$. The combined isotopic fractionation of all sources, α_{WT}, is calculated using the proportion of CH_4 removed by each sink (F) and their experimentally determined α values:

$$\alpha_{WT} = F_{OH} \cdot \alpha_{OH} + F_{soil} \cdot \alpha_{soil} + F_{strat} \cdot \alpha_{strat} + F_{MBL} \cdot \alpha_{MBL} \tag{3}$$

with

$$\sum F_{1-z} = 1 \tag{4}$$

It is useful to describe the isotopic offset (in ‰) between $\delta^{13}C_E$ and atmospheric $\delta^{13}CH_4$ caused by α_{WT} as the isotope separation factor ε_{WT}:

$$\varepsilon_{WT} \approx 10^3 \ln \alpha_{WT} \approx 10^3 (1 - \alpha_{WT}) \tag{5}$$

The individual values for F are not well constrained. They are commonly tuned to match the offset between measured atmospheric $\delta^{13}CH_4$ and bottom-up source scenarios. The greatest uncertainty concerns the MBL sink that has been estimated to account for ~5% of the total sink, i.e., F_{MBL} = 0.05 [*Allan et al.*, 2005]. However, because no direct evidence for the sink has been presented to date we will present alternative estimates for scenarios with and without an MBL sink. For the modern non-MBL estimate we adopt the values used by *Sowers et al.* [2005] with one modification. In order to compensate for lower stratospheric fractionation [*Wang et al.*, 2002], we increase soil uptake by 5 Tg/a to a total of 38 Tg/a, consistent with the preferred estimate of *Ridgwell et al.* [1999]. The resulting values are F_{OH} = 0.86, F_{soil} = 0.076, and F_{strat} = 0.07 (Figure 4). Accordingly, ε_{WT} indicates a ^{13}C enrichment of 7.4‰, which is also the value used by *Ferretti et al.* [2005] and *Sowers et al.* [2005]. The MBL scenario includes a 5% contribution from this sink with proportionally lower percentages for the other removal processes, resulting in F_{OH} = 0.817, F_{soil} = 0.072, F_{strat} = 0.067, and F_{MBL} = 0.05. In this case, ε_{WT} indicates a ^{13}C enrichment of 10.2‰.

[42] Changes in sink fractionation and magnitude in the past result from climate change and absence of anthropogenic influences. In the following, we present for each sink process estimates of F and α values. We can show that α values are unlikely to have changed significantly in the past, while the changes in F values had considerable impact on ε_{WT}. For reconstructions of the PIH we neglect climatic differences to the present. We try to quantify the effects of anthropogenic activity since the industrial revolution on atmospheric chemistry, vegetation, and soil properties and the impact on sink processes. Differences between LGM and PIH include climate, changes in ice-free land surface, and atmospheric chemistry. Climate models predict that the LGM was cooler by ~4.3°C on the global average [*Bush and Philander*, 1999]. For terrestrial environments, we use an average temperature difference of 7°C to be consistent with the vegetation reconstructions of *Collatz et al.* [1998]. Reconstructions for the YD are complicated by the fact that there are few specific studies of the CH_4 cycle and environmental parameters for this time. Here we assume that atmospheric methane concentration [CH_4] is an indicator for conditions that prevailed in regions relevant for the CH_4 cycle. Following this argument, environmental parameters were close to the intermediate values between PIH and LGM [*Brook et al.*, 2000] and we calculate ε_{WT} for the YD accordingly.

3.1. Hydroxyl Sink

[43] The photochemical abstraction reaction with OH· is the primary sink of atmospheric CH_4 and occurs mostly in the troposphere, where $O(^1D)$ and chlorine radicals (Cl·) contribute to a minor extent. The fractionation coefficient of the OH· reaction α_{OH} has been measured as 1.0054 ± 0.0009, independent of temperature between 0° and 80°C [*Cantrell et al.*, 1990]. *Saueressig et al.* [2001] determined α_{OH} with higher precision to be 1.0039 ± 0.0004. The loss rate of the OH· sink depends on temperature and [CH_4] and [OH·] [*Fung et al.*, 1991]. The fact that these three variables changed in the past did not necessarily affect F_{OH}. Instead, variations in [OH·] likely changed the atmospheric residence time of CH_4, which has no effect on $\delta^{13}CH_4$ under steady state conditions [*Tans*, 1997]. In this study, F_{OH} is set to balance variations in the other sinks, relative to total emissions of a given steady state scenario given by *Chappellaz et al.* [1993]. This is justified by the lack of unequivocal evidence for changes in [OH·] [e.g., *Staffelbach et al.*, 1991; *Martinerie et al.*, 1995], but could be simplistic in light of recent indications for a substantial [OH·] increase between LGM and PIH [*Valdes et al.*, 2005; *Kaplan et al.*, 2006].

3.2. Soil Uptake

[44] Soil uptake is based on diffusive flux of CH_4 into the soil and microbial consumption of CH_4. The associated α_{soil}

has been experimentally determined as 1.017 [*Snover and Quay*, 2000], 1.022 [*King et al.*, 1989; *Tyler et al.*, 1994] and 1.025 [*Reeburgh et al.*, 1997]. Case studies show that land conversion, agriculture and forestry affect CH_4 consumption of soils [*Steudler et al.*, 1996; *Del Grosso et al.*, 2000]. On a global scale, land use change has decreased soil uptake by ~10% since the PIH [*Ridgwell et al.*, 1999]. Soil uptake of CH_4 is controlled by diffusion [*Striegl*, 1993; *Tyler et al.*, 1994] and microbial oxidation rates [*Ridgwell et al.*, 1999]. Both processes are sensitive to $[CH_4]$ and the response of oxidation is nonlinear below soil concentrations of 300 ppbv [*Ridgwell et al.*, 1999]. While this barely affects present soil uptake, the impact increases with lower atmospheric $[CH_4]$. Using a process-based model, soil uptake in the PIH has been calculated as ~14 Tg/a, or 37% of the modern estimate [*Kaplan*, 2002].

[45] For the LGM we calculate a higher α_{soil} of 1.0272, according to the experimentally determined temperature dependence by *Tyler et al.* [1994]. The soil sink magnitude decreased because of (1) lower temperature (15% for a temperature drop of 7°C [*Yonemura and Yokozawa*, 2000]), (2) generally drier glacial conditions [*Yonemura and Yokozawa*, 2000] and (3) changes in ice-free surface area available for CH_4 uptake. The major restriction of the LGM soil sink is that $[CH_4]$ is only 50 ppbv higher than the linearity threshold for microbial kinetics [*Brook et al.*, 2000; *Ridgwell et al.*, 1999], so that most microbial communities are starved for CH_4. For this study we adopt the modeled LGM soil sink of ~0.6 Tg/a by *Kaplan* [2002].

[46] For the YD we infer the magnitude of the YD soil sink by scaling linearly to the findings of *Kaplan* [2002] for LGM and PIH, respectively. This gives a very conservative range from 0.9 to 9.3 Tg/a. Our preferred value of 6 Tg/a is derived from a power function fit for a crossplot of sink estimates [*Kaplan*, 2002] and $[CH_4]$ [*Brook et al.*, 2000] from LGM to present. We calculate α_{soil} = 1.0256 for a temperature decrease of 3.5°C relative to the PIH [*Tyler et al.*, 1994].

3.3. Stratospheric Sink

[47] Stratospheric removal occurs through a combination of OH·, $O(^1D)$ and Cl· and at present leads to tropospheric ^{13}C enrichment of CH_4 by 0.5–0.6‰ [*McCarthy et al.*, 2001]. At stratospheric temperatures around 225 K, α_{Cl} is between 1.073 [*Saueressig et al.*, 1995] and 1.070 [*Tyler et al.*, 2000] and $\alpha_{O(1D)}$ is 1.013 [*Saueressig et al.*, 2001]. The fraction of CH_4 removed by each reaction type, and therefore α_{strat}, varies with altitude and latitude. At higher elevation with lower $[CH_4]$ the higher fractionating sinks become more important. The observed correlation results in apparent α_{strat} between 1.0108 and 1.0204 [*Rice et al.*, 2003]. Within this range we adopt a value of 1.0133 that matches the magnitude of the stratospheric sink as modeled by *Wang et al.* [2002].

[48] Since the PIH, anthropogenic emissions of chlorocarbons increased [Cl·] strongly. *Wang et al.* [2002] model the effect on tropospheric $\delta^{13}CH_4$ and find ^{13}C depletion of ~0.4‰ for preindustrial conditions. We include this result by simply lowering α_{strat} for the PIH to 1.0082 although the variation in CH_4 removal largely occurred in the troposphere. However, the impact on ε_{WT} is captured accurately. The stratosphere in the PIH is up to 11°C warmer than today because of heat absorption caused by changes in photochemistry [*Martinerie et al.*, 1995]. This means a significant increase in reaction rate [*Michelsen and Simpson*, 2001] but does not necessarily translate into a higher sink magnitude, e.g., if Cl availability becomes limiting. The temperature increase would reduce α_{Cl} by 0.001 [*Tyler et al.*, 2000], which has a negligible effect on ε_{WT}. No $\delta^{13}CH_4$ changes caused by variations in the $O(^1D)$ reaction with CH_4 are considered throughout this study because its total modern effect on $\delta^{13}CH_4$ is only ~0.1‰ [*McCarthy et al.*, 2001] and any changes to this value can be neglected. We do not account for feedbacks in atmospheric chemistry, such as the depression of [Cl·] through CH_4 [*Rice et al.*, 2003], because even an unrealistic complete shutdown of the Cl sink would lower $\delta^{13}CH_4$ only by ~0.3‰. The magnitude of the stratospheric sink is scaled linearly to the total sink, which includes several assumptions such as an equal impact of $[CH_4]$ on all sinks in troposphere and stratosphere.

[49] There are no available data concerning changes in [Cl·] between LGM and PIH. Varying production of the precursor methyl chloride in ocean environments and biomass burning [*Wayne*, 1991], as well as higher ocean-atmosphere exchange at different wind patterns could have affected the natural source of Cl. However, these processes are hard to quantify, therefore we follow *Martinerie et al.* [1995] and assume no changes in [Cl·] between PIH and LGM. The total effect of the preindustrial stratospheric sink on tropospheric $\delta^{13}CH_4$ amounts only to ~0.3‰ so that the following processes can be neglected. First, a 6°C higher stratospheric temperature in LGM versus PIH [*Martinerie et al.*, 1995] with reduction of α_{Cl} by 0.0005 [*Tyler et al.*, 2000]. Second, a change in reaction rates with opposite sign in a colder troposphere and warmer stratosphere. Third, potential lowering of the apparent α_{strat} with increasing transport. Fourth, dependence of α_{strat} on $[CH_4]$ [*Rice et al.*, 2003]. The only change we make for the LGM and YD is to adjust the magnitude of the stratospheric sink proportionally to the total sink rate.

3.4. Chlorine Sink in the Marine Boundary Layer

[50] Recent studies suggest that at present ε_{WT} is ~2‰ higher than commonly assumed [*Allan et al.*, 2005]. The likely cause is the reaction of CH_4 and Cl· in the marine boundary layer (MBL). The amount of CH_4 removal seems to vary interannually in an estimated range between 13 and 38 Tg/a. Enhanced ε_{WT} due to ^{13}C enrichment in the MBL could explain discrepancies between atmospheric $\delta^{13}CH_4$ [*Ferretti et al.*, 2005] and bottom-up budgets for the PIH [*Chappellaz et al.*, 1993]. For reconstructions of the MBL sink we assume that there is no anthropogenic influence and hence no difference between present day and PIH other than linear scaling to $[CH_4]$. Potential climate induced changes of the MBL source are difficult to assess. Cl formation by sea spray [*Mayewski et al.*, 1997] and solar radiation on the southern ocean [*Berger*, 1978], both of which increase photolytic Cl· formation, are higher at the LGM. There is also evidence for locally, but not necessarily globally, increased marine productivity that provides organic Cl precursors [*Bender*, 2003]. Proxies for formation of dime-

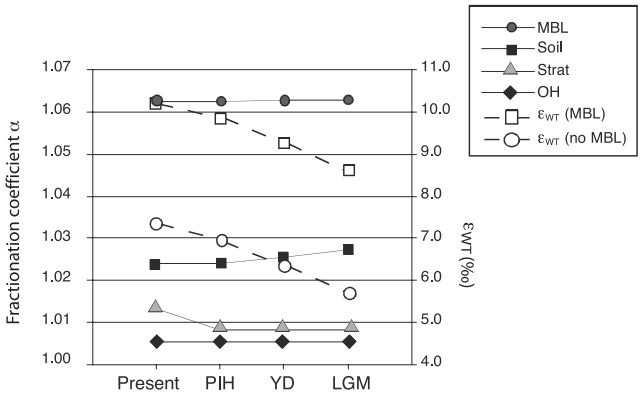

Figure 5. (left scale) Sink fractionation coefficients and (right scale) ε_{WT} from LGM to present. See text for discussion of uncertainties.

thylsulfide (also involved in Cl· formation) show opposite trends in records from Greenland and Antarctica [*Legrand et al.*, 1991; *Saltzman et al.*, 1997]. Currently, there is not enough evidence from ice cores or other sources to quantify past [Cl·] and consequently we do not consider climate related changes of the MBL sink magnitude, but scale the sink magnitude proportionally to [CH_4]. We adjust its α_{Cl} for lower T in YD and LGM with negligible impact on ε_{WT}.

3.5. Resulting Changes in Total Sink Fractionation

[51] We present two estimates for ε_{WT} in each climatic period because of uncertainties regarding the MBL sink. First, we list estimates that do not include an MBL sink. According to the information above, the fractions of the sink processes in the PIH were $F_{OH} \sim -0.857$, $F_{soil} \sim -0.073$, and $F_{strat} \sim -0.070$ (Figure 4). Using the same α_{OH} and α_{soil} for the PIH as at present, but lower α_{strat} to account for anthropogenic changes in [Cl·], we calculate $\varepsilon_{WT} \sim -7.0$‰ (Figure 5). The ~0.4‰ decrease relative to modern conditions is mostly due to the lower Cl· sink, whereas reduced soil uptake has little impact. For the LGM we calculate $F_{OH} \sim -0.925$, $F_{soil} \sim -0.005$ and $F_{strat} \sim -0.070$. α_{OH} and α_{strat} are the same as in the PIH, while α_{soil} is ~1.0272, because of lower temperature. ε_{WT} is then estimated at ~5.7‰. The significant difference to PIH and present is caused by the almost complete shutdown of soil uptake at low [CH_4]. For the YD we find a preferred solution (based on our best estimate of soil uptake) of $F_{OH} \sim -0.892$, $F_{soil} \sim -0.038$, and $F_{strat} \sim -0.070$. α_{soil} is calculated as ~1.0256, while α_{OH} and α_{strat} remain unchanged. The resulting ε_{WT} is ~6.4‰.

[52] Including the MBL sink we estimate that it contributed ~5% to the total source in all studied periods with proportionally lower F values for the other sinks. For α values as discussed above, the resulting ε_{WT} values are ~10.2‰ (present), ~9.9‰ (PIH), ~9.3‰ (YD) and ~8.6‰ (LGM). It is worth noting that the differences between the respective time periods are almost identical in the MBL and non-MBL scenarios.

[53] The reconstructions for ε_{WT} carry a large degree of uncertainty because they rely on various assumptions. The fractionation coefficients of individual sinks are reasonably well known, whereas their magnitudes are poorly constrained. For a comparison we use three scenarios with different sink estimates for the PIH from *Houweling et al.* [2000] (without early anthropogenic emissions considered in that study) and derive the associated F values. Together with our estimates for α values we calculate ε_{WT} values between ~6.5 and ~8.1‰. The ''Upper Limit'' scenario of *Houweling et al.* [2000] that produces a higher ε_{WT} than today requires an unrealistically large soil sink. The most likely scenario results in total sink fractionation of ~6.6‰, supporting that ε_{WT} was lower in the PIH than today. The difference to the PIH value derived above (~0.4‰) is similar to analytical precision for ice core $\delta^{13}CH_4$ measurements.

[54] We also test the sensitivity of ε_{WT} to the magnitude of individual sinks in the YD scenario. Varying the MBL sink by ±50%, which is equivalent to presently observed interannual variations [*Allan et al.*, 2005], changes ε_{WT} by ±1.5‰. Without better knowledge of the MBL sink ε_{WT} will remain poorly constrained. However, relative changes in ε_{WT} between different stages are expected to be less sensitive to these uncertainties if the MBL sink varies proportionately to [CH_4]. The soil sink magnitude for the YD is uncertain within 1 order of magnitude and the associated changes in sink fractionation are −0.7‰ to +0.4‰. Uncertainties in the magnitude of the stratospheric sink can be neglected, as they influence ε_{WT} by less than ±0.3‰ for a ±50% magnitude change.

[55] The major controls of past variations in ε_{WT} are the strong increase in α_{strat} from the PIH to present (Figure 5) and the magnitude of the soil sink (Figure 4). The stratospheric sink and its anthropogenic contribution is fairly well constrained by measurements [*Rice et al.*, 2003] and atmospheric chemistry models [*Wang et al.*, 2002]. Any natural, climate related changes of this sink are small by comparison and likely had a very minor impact on ε_{WT}. The soil sink is very sensitive to low [CH_4] in glacial times. This nonlinear response is the main control of ε_{WT} in preindustrial times and must be quantified using process-based models of soil uptake. The main unknown for the reconstruction of CH_4 sinks in the past is a possible Cl sink in the MBL. This process is inferred rather than directly measured for the modern system and seems to undergo significant short-term fluctuations [*Allan et al.*, 2005]. This fact, together with the potential for change induced by meteorology and biology in a glacial environment, does not currently allow for reliable reconstructions of the MBL sink.

[56] The combined changes lead to ε_{WT} for the LGM that is estimated to be ~1.7‰ lower that at present, which must be accounted for in budget reconstructions.

4. Conclusions

[57] The isotopic signatures of sources and sink fractionation change between modern and preindustrial times and over glacial cycles. Changes in the atmospheric CO_2 budget and shifting patterns of C_3 and C_4 vegetation between LGM, PIH, and present significantly change the $\delta^{13}C$ of the CH_4 precursor material of several source types. C_3–C_4–dependent sources are generally more ^{13}C rich in earlier time periods, as are total emissions. The contribution of

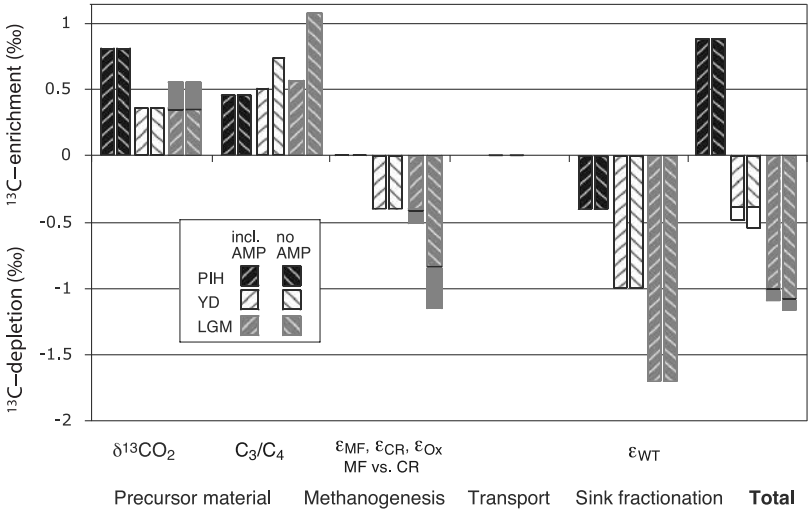

Figure 6. Changes of $\delta^{13}CH_4$ associated with various steps of the CH_4 cycle. All reconstructed values are relative to present-day numbers and represent best estimates. Estimates are given for each time period and budget scenarios with, and without, AMP emissions. Areas that are not hatched indicate the range between low and high estimates where applicable. MF stands for methyl fermentation; CR stands for carbonate reduction. See text for discussion of uncertainties.

these changes to glacial-interglacial shifts in atmospheric $\delta^{13}CH_4$ is minor. The magnitude of the change is specific for the emission budget and must be assessed in an iterative process when methane budgets are derived from $\delta^{13}CH_4$ paleodata.

[58] Our results regarding C_3-C_4 shifts generally support the assumption that emission rates, rather than $\delta^{13}CH_4$ of individual sources, are the main control for the stable carbon isotope ratio of atmospheric CH_4. It is important, however, that source scenarios have a high degree of sophistication as shown by the following example. With our presented bottom-up model we calculate ~2.6–3.0‰ ^{13}C depletion between LGM and PIH, which is largely caused by changing emissions in different wetland systems. In a top-down budget that distinguishes only a microbial, a thermogenic and a pyrogenic source, such a change must be interpreted as a strong relative decrease of geologic and wildfire emissions, overestimating their actual decline in our scenario at least threefold. This demonstrates that these simplistic budgets cannot describe variations in $\delta^{13}CH_4$ adequately. Even a generic wetland source with uniform $\delta^{13}CH_4$ for all latitudes would not allow for resolution of the changes, so that latitudinal wetland belts must be identified in budget scenarios.

[59] The potential impact of temperature on pathways of wetland CH_4 formation, their fractionation coefficients and consequently on atmospheric $\delta^{13}CH_4$ is difficult to quantify, but is likely large enough to affect ice core records between glacial and interglacial stages and must be accounted for in their interpretation. In contrast, field studies suggest that temperature induced change of the net to gross CH_4 production ratio in wetlands with large impact on $\delta^{13}CH_4$ is unlikely.

[60] This study also shows that total sink fractionation changes significantly in the past. The difference between the PIH and the present likely results in modest ^{13}C depletion of atmospheric CH_4 due to anthropogenic Cl emissions. For time periods with low $[CH_4]$, like the YD and LGM, ε_{WT} is smaller because the soil sink is decreased. This effect is large enough to affect ice core $\delta^{13}CH_4$. Differences in ε_{WT} between the various time periods are the same whether a MBL sink is considered or not.

[61] The individual and cumulative changes in atmospheric $\delta^{13}CH_4$ associated with various steps in the CH_4 cycle are shown in Figure 6. ^{13}C enrichment of precursor material and higher ^{13}C enrichment during methanogenesis and CH_4 loss partly cancel each other. The total estimated effect of environmental changes in the YD (~0.4‰ ^{13}C depletion) is of similar magnitude as current analytical precision of ice core $\delta^{13}CH_4$ measurements [*Ferretti et al.*, 2005]. The total change that we derive for the PIH (~0.8‰ ^{13}C enrichment) and LGM (~1–1.2‰ ^{13}C depletion), however, would be detectable in ice records. Our results suggest that the atmospheric ^{13}C enrichment observed in the late PIH is mostly caused by reorganization of the source-sink configuration while the environmental changes studied here make only a minor contribution. For full glacial conditions a substantial ^{13}C depletion of atmospheric CH_4 is expected, which is in contrast with the first available ice core $\delta^{13}CH_4$ data [*Sowers*, 2006; V. V. Petrenko, unpublished data, 2006]. The latter show ^{13}C enrichment by several permil relative to today, suggesting that the processes leading to depletion have either been overestimated in this study or are overcompensated by changes in relative emission rates. The conventional approach to interpret changes in $\delta^{13}CH_4$ as variations in source flux or atmospheric removal is largely justified, but budget reconstructions will be less accurate if changes in isotopic signatures of sources and sink fractionation are neglected.

[62] **Acknowledgments.** We thank Ed Brook for helpful discussions and Todd Sowers, as well as an anonymous reviewer, for valuable comments that strongly improved the manuscript. This work was supported by a

fellowship from DAAD (German Academic Exchange Service) (H.S.), Petroleum Research Fund of the American Chemical Society (H.S.), Canadian Foundation for Climate and Atmospheric Sciences CFCAS MAMMOTH Grant (M.J.W.), and NSERC Discovery Grant (M.J.W.).

References

Allan, W., D. C. Lowe, A. J. Gomez, H. Struthers, and G. W. Brailsford (2005), Interannual variation of ^{13}C in tropospheric methane: Implications for a possible atomic chlorine sink in the marine boundary layer, *J. Geophys. Res.*, *110*, D11306, doi:10.1029/2004JD005650.

Bellisario, L. M., J. L. Bubier, T. R. Moore, and J. P. Chanton (1999), Controls on CH_4 emissions from a northern peatland, *Global Biogeochem. Cycles*, *13*, 81–92.

Bender, M. (2003), Climate-biosphere interactions on glacial-interglacial timescales, *Global Biogeochem. Cycles*, *17*(3), 1082, doi:10.1029/2002GB001932.

Bergamaschi, P., et al. (2007), Satellite chartography of atmospheric methane from SCIAMACHYon board ENVISAT: 2. Evaluation based on inverse model simulations, *J. Geophys. Res.*, *112*, D02304, doi:10.1029/2006JD007268.

Berger, A. L. (1978), Long-term variations of caloric insolation resulting from the Earth's orbital elements, *Quat. Res.*, *9*, 139–167.

Bilek, R. S., S. C. Tyler, M. Kurihara, and K. Yagi (2001), Investigation of cattle methane production and emission over a 24-hour period using measurements of $\delta^{13}C$ and δD of emitted CH_4 and rumen water, *J. Geophys. Res.*, *106*, 15,405–15,413.

Blair, N. E., S. E. Boehme, and W. D. Carter Jr. (1993), The carbon isotope biogeochemistry of methane production in anoxic sediments: 1. Field observations, in *Biogeochemistry of Global Change*, edited by R. S. Oremland, pp. 574–593, Chapman and Hall, New York.

Botz, R., H. D. Pokojski, M. Schmitt, and M. Thomm (1996), Carbon isotope fractionation during bacterial methanogenesis by CO_2 reduction, *Org. Geochem.*, *25*, 255–262.

Bréas, O., C. Guillou, F. Reniero, and F. E. Wada (2001), The global methane cycle: Isotopes and mixing ratios, sources and sinks, *Isot. Environ. Health Stud.*, *37*, 257–379.

Brook, E. J., S. Harder, J. P. Severinghaus, E. J. Steig, and C. M. Sucher (2000), On the origin and timing of rapid changes in atmospheric methane during the last glacial period, *Global Biogeochem. Cycles*, *14*, 559–572.

Bush, A. B. G., and S. G. H. Philander (1999), The climate of the last glacial maximum: Results from a coupled atmosphere-ocean circulation model, *J. Geophys. Res.*, *104*, 24,509–24,525.

Cantrell, C. A., R. E. Shetter, A. H. McDaniel, J. G. Calvert, J. A. Davidson, D. C. Lowe, S. C. Tyler, R. J. Cicerone, and J. P. Greenberg (1990), Carbon kinetic isotope effect in the oxidation of methane by the hydroxyl radical, *J. Geophys. Res.*, *95*, 22,455–22,462.

Chanton, J. P. (2005), The effect of gas transport on the isotope signature of methane in wetlands, *Org. Geochem.*, *36*, 753–768.

Chanton, J. P., C. M. Rutkowski, C. C. Schwartz, D. E. Ward, and L. Boring (2000), Factors influencing the stable carbon isotopic signature of methane from combustion and biomass burning, *J. Geophys. Res.*, *105*, 1867–1877.

Chappellaz, J. A., I. Y. Fung, and A. M. Thompson (1993), The atmospheric CH_4 increase since the Last Glacial Maximum. (1). Source estimates, *Tellus, Ser B*, *45*, 228–241.

Collatz, G. J., J. A. Berry, and J. S. Clark (1998), Effects of climate and atmospheric CO_2 partial pressure on the global distribution of C_4 grasses: Present, past, and future, *Oecologia*, *114*, 441–454.

Cramer, W., et al. (1999), Comparing global models of terrestrial net primary productivity (NPP): Overview and key results, *Global Change Biol.*, *5*, 1–15.

Crutzen, P. J. E., E. Sanhueza, and C. A. M. Brenninkmeijer (2006), Methane production from mixed tropical savanna and forest vegetation in Venezuela, *Atmos. Chem. Phys. Discuss.*, *6*, 3093–3097.

DeBano, L. F., D. G. Neary, and P. F. Folliott (1998), *Fire's Effects on Ecosystems*, 333 pp., John Wiley, New York.

Del Grosso, S. J., et al. (2000), General CH_4 oxidation model and comparisons of CH_4 oxidation in natural and managed systems, *Global Biogeochem. Cycles*, *14*, 999–1019.

Dlugokencky, E. J., R. C. Myers, P. M. Lang, K. A. Masarie, A. M. Crotwell, K. W. Thoning, B. D. Hall, J. W. Elkins, and L. P. Steele (2005), Conversion of NOAA atmospheric dry air CH_4 mole fractions to a gravimetrically prepared standard scale, *J. Geophys. Res.*, *110*, D18306, doi:10.1029/2005JD006035.

Dueck, T. A., et al. (2007), No evidence for substantial aerobic methane emission by terrestrial plants: A ^{13}C-labelling approach, *New Phytol.*, *175*, 29–35, doi:10.1111/j.1469-8137.2007.02103.x.

Ehleringer, J. R., and R. K. Monson (1993), Evolutionary and ecological aspects of photosynthetic pathway variation, *Ann. Rev. Ecol. Syst.*, *24*, 411–439.

Ehleringer, J. R., T. E. Cerling, and B. R. Helliker (1997), C_4 photosynthesis, atmospheric CO_2, and climate, *Oecologia*, *112*, 285–299.

Etiope, G., and A. V. Milkov (2004), A new estimate of global methane flux from onshore and shallow submarine mud volcanoes to the atmosphere, *Environ. Geol.*, *46*, 997–1002.

Ferretti, D. F., et al. (2005), Unexpected changes to the global methane budget over the past 2000 years, *Science*, *309*, 1714–1717.

Fey, A., P. Claus, and R. Conrad (2004), Temporal change of ^{13}C isotopic signatures and methanogenic pathways in rice field soil incubated anoxically at different temperatures, *Geochim. Cosmochim. Acta*, *68*, 293–306.

Francey, R. F., C. E. Allison, D. M. Etheridge, C. M. Trudinger, I. G. Enting, M. Leuenberger, R. L. Langenfelds, E. Michel, and L. P. Steele (1999), A 1000-year high precision record of $\delta^{13}C$ in atmospheric CO_2, *Tellus, Ser. B*, *51*, 170–193.

François, L. M., C. Delire, P. Warnant, and G. Munhoven (1998), Modelling the glacial-interglacial changes in the continental biosphere, *Global Planet. Change*, *16–17*, 37–52.

Fung, I. Y., J. John, J. Lerner, E. Matthews, M. Prather, L. P. Steele, and P. J. Fraser (1991), Three-dimensional model synthesis of the global methane cycle, *J. Geophys. Res.*, *96*, 13,033–13,065.

Games, L. M., and J. M. Hayes (1976), On the mechanisms of CO_2 and CH_4 production in natural anaerobic environments, in *Environmental Biogeochemistry,* vol. 1, *Carbon, Nitrogen, Phosphorus, Sulphur and Selenium Cycles*, edited by J. O. Nriagu, pp. 51–73, Ann Arbor Sci., Ann Arbor, Mich.

Hallgren, W. S., and A. J. Pitman (2000), The uncertainty in simulations by a global biome model (BIOME3) to alternative parameter values, *Global Change Biol.*, *6*, 483–495.

Hao, W. M., and D. E. Ward (1993), Methane production from global biomass burning, *J. Geophys. Res.*, *98*, 20,657–20,661.

Harrison, S. P., and C. I. Prentice (2003), Climate and CO_2 controls on global vegetation distribution at the Last Glacial Maximum: Analysis based on palaeovegetation data, biome modeling and paleoclimate simulations, *Global Change Biol.*, *9*, 983–1004.

Heimann, M., et al. (1998), Evaluation of terrestrial carbon cycle models through simulations of the seasonal cycle of atmospheric CO_2: First results of a model intercomparison study, *Global Biogeochem. Cycles*, *12*, 1–24.

Hein, R., P. J. Crutzen, and M. Heimann (1997), An inverse modeling approach to investigate the global atmospheric methane cycle, *Global Biogeochem. Cycles*, *11*, 43–76.

Houweling, S., F. Dentener, and J. Lelieveld (2000), Simulation of preindustrial atmospheric methane to constrain the global source strength of natural wetlands, *J. Geophys. Res.*, *105*, 17,243–17,255.

Houweling, S., T. Röckmann, I. Aben, F. Keppler, M. Krol, J. F. Meirink, E. Dlugokencky, and C. Frankenberg (2006), Atmospheric constraints on global emissions of methane from plants, *Geophys. Res. Lett.*, *33*, L15821, doi:10.1029/2006GL026162.

Kaplan, J. O. (2002), Wetlands at the Last Glacial Maximum: Distribution and methane emissions, *Geophys. Res. Lett.*, *29*(6), 1079, doi:10.1029/2001GL013366.

Kaplan, J. O., G. Folberth, and D. A. Hauglustaine (2004), Ice age methane revisited: Oceans, lightning, and the steady wetland source, *Eos Trans. AGU*, *85*(17), Jt. Assem. Suppl., Abstract GC21A-18.

Kaplan, J. O., G. Folberth, and D. A. Hauglustaine (2006), Role of methane and biogenic volatile organic compound sources in late glacial and Holocene fluctuations of atmospheric methane concentrations, *Global Biogeochem. Cycles*, *20*, GB2016, doi:10.1029/2005GB002590.

Keppler, F., J. T. G. Hamilton, M. Braß, and T. Röckmann (2006), Methane emissions from terrestrial plants under aerobic conditions, *Nature*, *439*, 187–191.

King, S. L., P. D. Quay, and J. M. Lansdowne (1989), The $^{13}C/^{12}C$ kinetic isotope effect for soil oxidation of methane at ambient atmospheric concentrations, *J. Geophys. Res.*, *94*, 18,273–18,277.

Kirschbaum, M. U. K., et al. (2006), A comment on the quantitative significance of aerobic methane release by plants, *Funct. Plant Biol.*, *33*, 521–530.

Kvenvolden, K. A., and B. W. Rogers (2005), Gaia's breath—Global methane exhalations, *Mar. Petrol. Geol.*, *22*, 579–590.

Legrand, M. R., C. Feniet-Saigne, E. S. Saltzman, C. Germain, N. I. Barkov, and V. N. Petrov (1991), Ice-core record of oceanic emissions of dimethylsulfide during the last glacial cycle, *Nature*, *350*, 144–146.

Levin, I., P. Bergamaschi, H. Dörr, and D. Trapp (1993), Stable isotopic signature of methane from major sources in Germany, *Chemosphere*, *26*, 161–177.

MacDonald, M. G., D. W. Beilman, K. V. Kremenetski, Y. Sheng, L. C. Smith, and A. A. Velichko (2006), Rapid early development of circumarctic peatlands and atmospheric CH_4 and CO_2 variations, *Science*, *314*, 285–288.

Marino, B. D., M. B. McElroy, R. J. Salawitch, and G. W. Spaulding (1992), Glacial-to-interglacial variations in the carbon isotopic composition of atmospheric CO_2, *Nature*, *357*, 461–466.

Martinerie, P., G. P. Brasseur, and C. Granier (1995), The chemical composition of ancient atmospheres: A model study constrained by ice core data, *J. Geophys. Res.*, *100*, 14,291–14,304.

Mayewski, P. A., L. D. Meeker, M. S. Twickler, S. Whitlow, Q. Yang, W. B. Lyons, and M. Prentice (1997), Major features and forcing of high-latitude Northern Hemispheric atmospheric circulation using a 110,000-year-long glaciochemical series, *J. Geophys. Res.*, *102*, 26,345–26,366.

McCarthy, M. C., P. Connell, and K. A. Boering (2001), Isotopic fractionation of methane in the stratosphere and its effect on free tropospheric isotopic compositions, *Geophys. Res. Lett.*, *28*, 3657–3660.

Metges, C., K. Kempe, and H. L. Schmidt (1990), Dependence of the carbon-isotope contents of breath carbon dioxide, milk, serum, and rumen fermentation products on the $\delta^{13}C$ value of food in dairy cows, *Br. J. Nutr.*, *63*, 187–196.

Michelsen, H. A., and W. R. Simpson (2001), Relating state-dependent cross sections to non-Arrhenius behavior for the Cl + CH_4 reaction, *J. Phys. Chem. A*, *105*, 1476–1488.

Miller, J. B., K. A. Mack, R. Dissly, J. W. C. White, E. J. Dlugokencky, and P. P. Tans (2002), Development of analytical methods and measurements of $^{13}C/^{12}C$ in atmospheric CH_4 from the NOAA Climate Monitoring and Diagnostics Laboratory Global Air Sampling Network, *J. Geophys. Res.*, *107*(D13), 4178, doi:10.1029/2001JD000630.

Moosavi, S. C., and P. M. Crill (1998), CH_4 oxidation by tundra wetlands as measured by a selective inhibitor technique, *J. Geophys. Res.*, *103*, 29,093–29,106.

Parsons, A. J., P. C. D. Newton, H. Clark, and F. M. Kelliher (2006), Scaling methane emissions from vegetation, *Trends Ecol. Evol.*, *21*, 423–424.

Prather, M., et al. (2001), Atmospheric chemistry and greenhouse gases, in *Climate Change 2001: The Scientific Basis*, edited by J. T. Houghton, et al., Cambridge Univ. Press, New York.

Prentice, I. C., M. T. Sykes, M. Lautenschlager, S. P. Harrison, O. Denissenko, and P. J. Bartlein (1993), Modelling global vegetation patterns and terrestrial carbon storage at the Last Glacial Maximum, *Global Ecol. Biogeogr. Lett.*, *3*, 67–76.

Reeburgh, W. S., A. I. Hirsch, F. J. Sansone, B. N. Popp, and T. M. Rust (1997), Carbon kinetic isotope effect accompanying microbial oxidation of methane in boreal forest soils, *Geochim. Cosmochim. Acta*, *61*, 4761–4767.

Rice, A. L., S. C. Tyler, M. C. McCarthy, K. A. Boering, and E. Atlas (2003), Carbon and hydrogen isotopic compositions of stratospheric methane: 1. High-precision observations from the NASA ER-2 aircraft, *J. Geophys. Res.*, *108*(D15), 4460, doi:10.1029/2002JD003042.

Ridgwell, A. J., S. J. Marshall, and K. Gregson (1999), Consumption of atmospheric methane by soils: A process-based model, *Global Biogeochem. Cycles*, *13*, 59–70.

Ruddiman, W. F., and J. S. Thomson (2001), The case for human causes of increased atmospheric CH_4 over the last 5000 years, *Quat. Sci. Rev.*, *20*, 1769–1777.

Rust, F. E. (1981), ($\delta^{13}C/^{12}C$) of ruminant methane and its relationship to atmospheric methane, *Science*, *211*, 1044–1046.

Saltzman, E. S., P. Y. Whung, and P. A. Mayewski (1997), Methanesulfonate in the Greenland Ice Sheet Project 2 ice core, *J. Geophys. Res.*, *102*, 26,649–26,658.

Sanhueza, E., and L. Donoso (2006), Methane emissions from tropical *Trachypogon sp.* grasses, *Atmos. Chem. Phys. Discuss.*, *6*, 6841–6852.

Saueressig, G., P. Bergamaschi, J. N. Crowley, H. Fischer, and G. W. Harris (1995), Carbon kinetic isotope effect in the reaction of CH_4 with Cl atoms, *Geophys. Res. Lett.*, *22*, 1225–1228.

Saueressig, G., J. N. Crowley, P. Bergamaschi, C. Bruehl, C. A. Brenninkmeijer, and H. Fischer (2001), Carbon 13 and D kinetic isotope effects in the reactions of CH_4 with O (^1D) and OH: New laboratory measurements and their implications for the isotopic composition of stratospheric methane, *J. Geophys. Res.*, *106*, 23,127–23,138.

Schaefer, H. (2005), Stable carbon isotopic composition of methane from ancient ice samples, Ph.D. thesis, 191 pp., Univ. of Victoria, Victoria, B.C., Canada.

Schaefer, H., and M. J. Whiticar (2007), Measurement of stable carbon isotope ratios of methane in ice samples, *Org. Geochem.*, *38*, 216–226, doi:10.1016/j.orggeochem.2006.10.006.

Schaefer, H., M. J. Whiticar, E. J. Brook, V. V. Petrenko, D. F. Ferretti, and J. P. Severinghaus (2006), Ice record of $\delta^{13}C$ for atmospheric CH_4 across the Younger Dryas-Preboreal transition, *Science*, *313*, 1109–1112.

Schulze, E., S. Lohmeyer, and W. Giese (1998), Determination of $^{13}C/^{12}C$-ratios in rumen produced methane and CO_2 of cows, sheep and camels, *Isot. Environ. Health Stud.*, *34*, 75–79.

Segers, R. (1998), Methane production and methane consumption: A review of processes underlying wetland methane fluxes, *Biogeochemistry*, *41*, 23–51.

Smith, H. J., H. Fischer, M. Wahlen, D. Mastroianni, and B. Deck (1999), Dual modes of the carbon cycle since the Last Glacial Maximum, *Nature*, *400*, 248–250.

Snover, A. K., and P. D. Quay (2000), Hydrogen and carbon kinetic isotope effects during soil uptake of atmospheric methane, *Global Biogeochem. Cycles*, *14*, 25–39.

Sowers, T. A. (2006), Methane isotope records spanning the last 160 kyr: Correlations and conundrums, *Eos Trans. AGU*, *87*(52), Fall Meet. Suppl., Abstract U33C-04.

Sowers, T., S. Bernard, O. Aballain, J. A. Chappellaz, J.-M. Barnola, and T. Marik (2005), Records of the $\delta^{13}C$ of atmospheric CH_4 over the last 2 centuries as recorded in Antarctic snow and ice, *Global Biogeochem. Cycles*, *19*, GB2002, doi:10.1029/2004GB002408.

Staffelbach, T., A. Neftel, B. Stauffer, and D. Jacob (1991), A record of the atmospheric methane sink from formaldehyde in polar ice cores, *Nature*, *349*, 603–605.

Steudler, P. M., J. M. Melillo, B. J. Feigl, C. Neill, M. C. Piccolo, and C. C. Cerri (1996), Consequence of forest-to-pasture conversion on CH_4 fluxes in the Brazilian Amazon Basin, *J. Geophys. Res.*, *101*, 18,547–18,554.

Stevens, C. M., and A. Engelkemeir (1988), Stable carbon isotopic composition of methane from natural and anthropogenic sources, *J. Geophys. Res.*, *93*, 725–733.

Still, C. J., J. A. Berry, G. J. Collatz, and R. S. DeFries (2003), Global distribution of C_3 and C_4 vegetation: Carbon cycle implications, *Global Biogeochem. Cycles*, *17*(1), 1006, doi:10.1029/2001GB001807.

Striegl, R. G. (1993), Diffusional limits to the consumption of atmospheric methane by soils, *Chemosphere*, *26*, 715–720.

Tans, P. P. (1997), A note on isotopic ratios and the global atmospheric methane budget, *Global Biogeochem. Cycles*, *11*, 77–81.

Tyler, S. C., P. R. Zimmerman, C. Cumberbatch, J. P. Greenberg, C. Westberg, and J. P. E. C. Darlington (1988), Measurements and interpretation of $\delta^{13}C$ of methane from termites, rice paddies, and wetlands in Kenya, *Global Biogeochem. Cycles*, *2*, 341–355.

Tyler, S. C., P. M. Crill, and G. W. Brailsford (1994), $^{13}C/^{12}C$ fractionation of methane during oxidation in a temperate forested soil, *Geochim. Cosmochim. Acta*, *58*, 1625–1633.

Tyler, S. C., H. O. Ajie, A. L. Rice, R. J. Cicerone, and E. C. Tuazon (2000), Experimentally determined kinetic isotope effects in the reaction of CH_4 with Cl: Implications for atmospheric CH_4, *Geophys. Res. Lett.*, *27*, 1715–1718.

Valdes, P. J., D. J. Beerling, and C. E. Johnson (2005), The ice age methane budget, *Geophys. Res. Lett.*, *32*, L02704, doi:10.1029/2004GL021004.

van Huissteden, J. (2004), Methane emission from northern wetlands in Europe during oxygen isotope stage 3, *Quat. Sci. Rev.*, *23*, 1989–2005.

Walter, B. P., and M. Heimann (2000), A process-based, climate-sensitive model to derive methane emissions from natural wetlands: Application to five wetland sites, sensitivity to model parameters, and climate, *Global Biogeochem. Cycles*, *14*, 745–765.

Wang, J. S., M. B. McElroy, C. M. Spivakovsky, and D. B. A. Jones (2002), On the contribution of anthropogenic Cl to the increase in $\delta^{13}C$ of atmospheric methane, *Global Biogeochem. Cycles*, *16*(3), 1047, doi:10.1029/2001GB001572.

Wayne, R. P. (1991), *Chemistry of Atmospheres*, 447 pp., Calendon, Oxford, U. K.

Whiticar, M. J. (1990), A geochemical perspective of natural gas and atmospheric methane, *Org. Geochem.*, *16*, 531–547.

Whiticar, M. J. (1996), Isotope tracking of microbial methane formation and oxidation, in *Cycling of Reduced Gases in the Hydrosphere*, edited by D. D. Adams, P. M. Crill, and S. P. Seitzinger, *Mitt. Int. Verein. Limnol.*, vol. 23, pp. 39–54, Schweizerbart'sche, Stuttgart, Germany.

Whiticar, M. J. (1999), Carbon and hydrogen isotope systematics of bacterial formation and oxidation of methane, *Chem. Geol.*, *161*, 291–314.

Whiticar, M. J. (2000), Can stable isotopes and global budgets be used to constrain atmospheric methane budgets?, in *Atmospheric Methane, its Role in the Global Environment*, edited by M. A. K. Khalil, pp. 63–85, Springer, Berlin.

Whiticar, M. J., and E. Faber (1986), Methane oxidation in sediment and water column environments—Isotopic evidence, *Org. Geochem.*, *10*, 759–768.

Whiticar, M. J., and H. Schaefer (2007), Constraining past global tropospheric methane budgets with carbon and hydrogen isotope ratios in ice, *Philos. Trans. R. Soc. London, Ser. A*, *365*, 1793–1828, doi:10.1098/rsta.2007.2048.

Whiticar, M. J., E. Faber, and M. Schoell (1986), Biogenic methane formation in marine and freshwater environments: CO_2 reduction vs. acetate fermentation-isotopic evidence, *Geochim. Cosmochim. Acta*, *50*, 693–709.

Wright, H. A., and A. W. Bailey (1982), *Fire Ecology, United States and Southern Canada*, 501 pp., John Wiley, New York.

Wunsch, C. (2006), Abrupt climate change: An alternative view, *Quat. Res.*, *65*, 191–203.

Yonemura, S., and M. Yokozawa (2000), A process-based model for the global estimation of CH_4– and CO-uptake strengths by soils, *World Res. Rev.*, *12*, 149–170.

Zimmerman, P. R., J. P. Greenberg, S. O. Wandiga, and P. J. Crutzen (1982), Termites, a potentially large source of atmospheric methane, carbon dioxide, and molecular hydrogen, *Science*, *218*, 563–565.

H. Schaefer, Laboratoire de Glaciologie et Géophysique de l'Environnement, 54 rue Molière, Domaine Universitaire B.P. 96, F-38402 St. Martin d'Hères, France. (hinrich@lgge.obs.ujf-grenoble.fr)

M. J. Whiticar, School of Earth and Ocean Sciences, University of Victoria, P.O. Box 3055, Victoria, BC, Canada V8W 3P6.